Fundamental and Formation Aspects of Slag Freeze Linings: A Review

Inge Bellemans[1,*], Johan Zietsman[2,3], Kim Verbeken[1]

[1]Department of Materials, Textiles and Chemical Engineering, Ghent University, Techlane Ghent Science Park, Technologiepark 46, Zwijnaarde, 9052, Ghent, Belgium

[2]Department of Materials Science and Metallurgical Engineering, University of Pretoria, Pretoria, South Africa

[3]Ex Mente Technologies, Pretoria, South Africa

Correspondence to Inge Bellemans. Email: inge.bellemans@ugent.be

Graphical Abstract

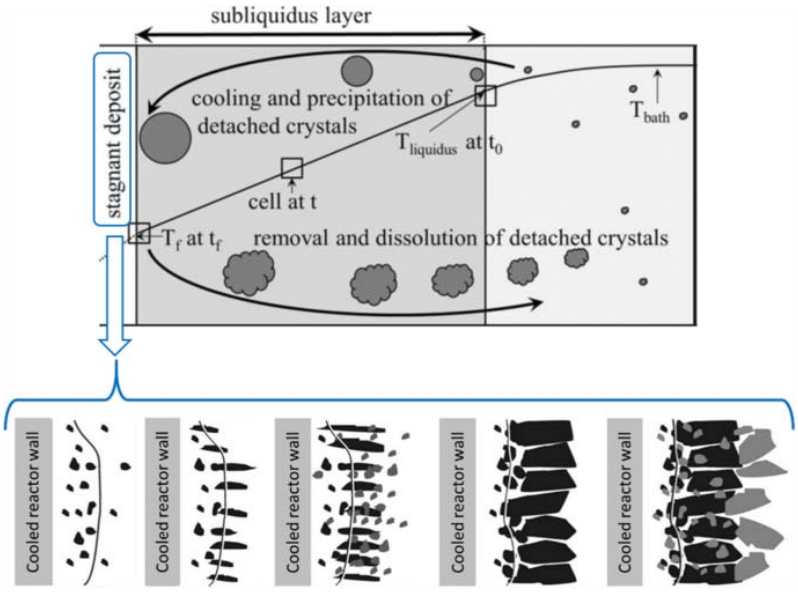

Abstract

Traditionally, pyrometallurgical reactors are lined on the inside with refractory materials. Some of the high-temperature phases are aggressive towards the furnace lining, requiring periodic repair or replacement of the lining. The freeze-lining concept, however, involves the deliberate formation of a layer of solidified bath material on the inner walls of the reactor lining. This self-repairing freeze lining can protect the reactor lining from corrosive attack by the liquid phases. Hence, this can be a solution for the periodically required lining replacement. However, the existing somewhat limited knowledge is mostly based on primary metal production systems, and future applications (with secondary feed materials for recycling purposes) will require more fundamental knowledge on the influencing parameters. This review collects the current knowledge regarding freeze linings. The various methods used to experimentally investigate freeze-lining phenomena experimentally are discussed. Then the generally accepted mechanism controlling freeze-lining formation is presented, followed by a listing of various influencing parameters. Next, the various mathematical models and approaches used to

describe freeze-lining thickness are introduced. The remaining challenges conclude this review.

Keywords: Freeze lining; Formation; Microstructure; Pyrometallurgy; Slags

Introduction

Context of Freeze Lining in Pyrometallurgy

In pyrometallurgy, metals are extracted from ores or scrap by high-temperature processes. Usually, the main phase is the liquid alloy phase, but besides this phase, there are also other phases: solid and liquid metal oxide solutions, called slag, and liquid metal sulfide solutions, called matte. The furnace's steel shell is conventionally covered with a refractory lining, typically an oxide material that can withstand high temperatures. This lining protects the shell from contact with the liquid phases at the high working temperatures. Due to physical, thermal, and chemical interaction between the refractory and the baths, the refractory degrades over time [1], eventually leading to furnace shutdown to reline the furnace [2]. When the lining is in direct contact with the mostly liquid slag, while the slag is saturated in the primary phase of the refractory material, the degradation can be kept to a minimum. Since the slag is saturated, it will not wear the refractory lining, or it will degrade it slowly. In the conventional concept, the refractory acts as a continuously diminishing protective layer. For this, typically thick refractory masses are used to withstand degradation and erosion as much as possible, but the degradation occurs anyway, leading to either high maintenance or breakouts.

In the metallurgical industry, a trend can be observed towards higher process intensities. This includes increases in both process temperatures and bath agitation to improve thermodynamics and kinetics of the reactions, respectively, and results in higher production rates. These conditions, however, pose more severe demands on the reactors and result in faster degradation of the refractory lining [3]. This faster degradation in turn results in more shutdowns to reline the furnace, which cost energy, time, and money.

In addition, as the demand for metals is increasing, the quantity and purity of the available ores are decreasing. The amount of waste keeps increasing and recycling becomes more important for a more sustainable and circular economy. The scrap can consist of a bulk metallic fraction such as iron or aluminum, but it can also be electronic waste, which contains several noble and rare-earth metals. The necessary new and more efficient processes to produce and recycle materials result in an evolution towards more complex and corrosive liquid phases. For example, some slags can become very aggressive towards the furnace lining, requiring more frequent relining [3]. Moreover, in several reactors with very corrosive liquids, long service life can only be achieved by the formation of a solid layer of slag or alloy on the furnace side wall as protection for the refractory [4].

Using freeze linings (a layer of solidified bath material, deliberately formed on the reactor wall inner surfaces, providing protection from the corrosive liquid slags) can be a solution for these situations because freeze linings have a self-repairing nature. For very corrosive systems, operation with a freeze lining is the only option. With the self-repairing character, no or less

relining of the whole furnace is required if a freeze lining is present. Note that the refractory walls still come into contact with liquid slag in the taphole areas and in the tidal zone (the zone of the interface between the slag and alloy baths). It is, therefore, still necessary to repair tapholes from time to time. But still, the use of a freeze lining reduces furnace downtime, and the corresponding costs and freeze-lining concepts can also be used in the taphole design [5]. This increases the sustainability as more diverse input streams can be used.

Historical Evolution

In the past, linings of small furnaces were considered to be consumable, and provision was made for regular replacement. The lining of the furnace was taken to be a receptacle with the only purpose to contain the molten materials [2]. As mentioned above, for some processes, no refractory-lining material exists for containment and freeze-lining operation can make such processes feasible. This is the case:

- Aluminum production cells: aluminum oxide is electrochemically reduced from a cryolite melt through electrolysis with carbon electrodes [6,7,8]. The electrolyte has a very corrosive nature. Because no other material than frozen cryolite can withstand the harsh conditions, it is necessary to maintain a protective layer of frozen electrolyte, called, 'side freeze' or 'side ledge,' on the lining [9]. Accurate control of the side ledge thickness and heat transfer of the side ledge is fundamental for stable process operation, i.e., stable bath temperature and bath composition [10].
- Ilmenite ($FeTiO_3$) smelting: high-titanium slag is produced by smelting ilmenite concentrate together with a carbonaceous reductant in AC and DC electric furnaces. The slag is very corrosive towards the refractory material. Besides the slag, also pig iron is produced, but the slag is the main product of the process. Because the subsequent fluidized-bed chlorination, used to manufacture pigment from the slag, can only tolerate small amounts of especially CaO and MgO [11,12,13], no fluxing additions are possible. Therefore, ilmenite smelters are operated with a freeze lining of solidified slag [14].

In the literature on aluminum cells, the term 'freeze lining' is never used, whereas the ilmenite smelting was developed after the term had been introduced. So when was the term first introduced?

In November 1980, a furnace breakout occurred in a submerged arc furnace (the M12 furnace at Metalloys [15], started up in July 1978). The breakout resulted from the thermal degradation of the carbonaceous lining material. After this event, the idea was launched that a 'natural' lining could be used, by which the process could be contained, but which also protected the hot face of the carbonaceous lining. In this way, there would theoretically be no degradation of the carbonaceous lining material. At that point in time, the concept 'freeze lining' was claimed 'new and not yet available,' although the side ledge formation in aluminum cells could be interpreted as a precursor.

After an initial impending failure of the lining four years into the operation, the first signs of significant degradation of the lining became evident in the beginning of 1999, i.e., after 18 years of operation. Later, in 2000, Kojo et al. [16] gave an account showing that the first water-cooled furnace construction, via vertical cooling elements in the refractory wall, in a flash smelting furnace already took place in 1950.

Nowadays, the following industries have been using freeze linings, as reported in literature:

- Aluminum cells [6,7,8]
- Ilmenite ($FeTiO_3$) smelting [11,12,13,14]
- Ferroalloy (ferromanganese, silicomanganese, ferrochrome) production [17, 18]
- Zinc fuming processes [10, 19,20,21]
- Copper smelting processes [22,23,24]
- Lead blast furnaces [25, 26]
- Platinum group metal smelting [27, 28]
- Submerged arc furnaces for both smelting and slag-cleaning applications [2, 18, 29, 30]

Most knowledge regarding freeze linings is based on experience in primary industries such as ferroalloys, ilmenite smelting, and aluminium production, which do not encounter frequently and significantly varying feed streams, as is usual in recycling/secondary industries. To be able to extend to more complex systems and phases, a more fundamental understanding of freeze linings and their influencing parameters is required.

Principle

A freeze lining is the result of a thermal balance between heat transfer from the bath to the lining and heat transfer through the lining. At steady state, the heat flow rate through the freeze lining will also be the same as the heat flow rate through the reactor wall and the heat flow rate going towards the cooling medium (Eq. (1)) [4, 31].

$$\dot{Q}_{\text{bath}} = \dot{Q}_{\text{fl}} = \dot{Q}_{\text{wall}} = \dot{Q}_{\text{coolant}}. \tag{1}$$

With the following expressions (Eqs. (2)-(5)) based on a straight wall assumption,

$$\dot{Q}_{\text{bath}} = h_{\text{bath}} \cdot A_{\text{bath}} \cdot (T_{\text{bath}} - T_{\text{f}}), \tag{2}$$

$$\dot{Q}_{\text{fl}} = \frac{k_{\text{fl}} \cdot A_{\text{fl}}}{X_{\text{fl}}} (T_{\text{f}} - T_{\text{wall,1}}), \tag{3}$$

$$\dot{Q}_{\text{wall}} = \frac{T_{\text{wall,1}} - T_{\text{wall,2}}}{R_{\text{wall}}}, \tag{4}$$

$$\dot{Q}_{\text{coolant}} = h_{\text{coolant}} \cdot A_{\text{wall}} \cdot (T_{\text{wall,2}} - T_{\text{coolant}}). \tag{5}$$

where h_{bath} [W/m^2 K] is the convection coefficient from the bath to the freeze lining, A_{bath} [m^2] the area normal to the direction of the heat transfer at the solid/liquid interface, T_{bath} [K] the bath temperature, T_{f} [K] the temperature at the interface between the stagnant deposit and the bath, k_{fl} [W/m K] the thermal conductivity of the freeze lining, A_{fl} [m^2] the area of the freeze layer, X_{fl} [m] the thickness of the freeze layer, $T_{\text{wall,1}}$ [K] the interface temperature between the freeze lining and reactor wall, $T_{\text{wall,1}}$ [K] the interface temperature between the reactor wall and the coolant, R_{wall} [K/W] the thermal resistance of the furnace wall (including the refractory and steel shell and defined below), and h_{coolant} [W/m^2 K], A_{wall} [m^2] the outside wall area and T_{coolant} [K] the coolant temperature. R_{wall} is defined in Eq. (6) as follows:

$$R_{\text{wall}} = \sum \frac{X_i}{k_i A_i}. \tag{6}$$

where X_i [m] is the thickness of the furnace wall component, k_i [W/m K] the thermal conductivities of the various furnace wall materials, and A_i [m^2] the area of the furnace wall through which the heat flows. In steady state and if it is assumed that the cross-section areas of all components are the same, the thickness of the freeze lining can be estimated as described in Eq. (7):

$$X_{\text{fl}} = \left(\frac{k_{\text{fl}}}{h_{\text{bath}}}\right) \cdot \left(\frac{T_{\text{f}} - T_{\text{coolant}}}{T_{\text{bath}} - T_{\text{f}}}\right) - \left(k_{\text{fl}} \sum \frac{X_i}{k_i}\right). \tag{7}$$

The equation shows the dependence of freeze-lining thickness on superheat ($T_{\text{bath}} - T_{\text{f}}$) and the various heat transfer coefficients and thermal conductivities. Furthermore, the equations show that both the steady-state thickness of the lining and the rate of heat loss through it depend on the interface temperature [32].

Nelson and Hundermark [5] gave some remarks based on the steady-state heat transfer illustrating that a stable freeze lining can only be formed for slag systems, i.e., there is no equivalent for liquid matte. The reason goes back to the physical properties of matte versus those of slag, resulting in higher heat fluxes in matte systems. In this case, an unprotected cooler in contact with such superheated matte can rapidly lead to hot-face temperatures rising to where the cooler material, typically copper, just melts.

Critical in using freeze linings is the stable deposit formation with an optimum thickness (too thick layers decrease the reactor volume and too thin layers result in excessive heat losses and frequent detachment of the freeze lining) [3]. When using a freeze-lining concept, achieving only a ‘partial’ and/or ‘periodic’ freeze lining is unwanted, as it results in considerably more dangerous operating conditions, than on a traditional design concept [5].

At steady state, the specific heat extraction rate through the furnace wall is solely determined by the convection coefficient from the bath to the sidewall and by the difference in bath temperature and the interface temperature between the bath and freeze lining. These parameters are mostly set for a certain system, and hence, a cooling design needs to be used to extract this steady-state heat flux. It is also clear that increasing the process intensities through an increase of bath temperature or convection will both increase the heat input from the bath to the wall and the heat extraction through the wall. This means that intensive processes require cooling systems that can extract high heat fluxes [3].

If adequate cooling is present, it has been observed that it is quite easy to form and maintain slag freeze linings from even superheated slag. Even a thin layer (of several mm thickness) can provide a sufficient thermal resistance to lower hot-face temperatures [5]. Using high-conductivity cooling blocks and refractories and/or insertion of high-conductivity rods in the freeze lining will increase the steady-state freeze-lining thickness but will not affect the heat removal through the furnace wall. If more air gaps between the different layers of the wall are present or if less conductive refractory materials are used, the thermal resistances increase, and the steady-state freeze-lining thickness will decrease. Hence, a wall design should promote good thermal contact between the layers so that a sufficient freeze-lining thickness is assured [3].

Any disruption, such as local mechanical failure or a change in bath composition, results in a non-steady-state solidification or dissolution of the freeze lining until the thermal balance is restored. The rate of heat input ($\dot{Q}$ in W) from the superheated bath together with the latent heat of fusion balance out the rate of heat removal through the cooled furnace wall as shown in Eq. (8) [3, 31, 33]:

$$\dot{Q}_{\text{bath}} + \dot{Q}_{\text{fusion}} = \dot{Q}_{\text{wall}}. \tag{8}$$

With

$$\dot{Q}_{\text{fusion}} = \rho \cdot H_{\text{f}} \cdot \frac{dX_{\text{fl}}}{dt} \cdot A_{\text{bath}}, \tag{9}$$

where ρ [kg/m^3] is the density of the freeze lining and H_{f} [J/kg] the specific latent heat of fusion. The latent heat of fusion flux $\dot{Q}_{\text{fusion}}$ is zero in steady state, in which case the thickness of the freeze-lining X_{fl} is constant over time [3].

The self-healing characteristics of a freeze lining are visible in Eq. (8): any disturbance in the heat flow rates $\dot{Q}_{\text{bath}}$ or $\dot{Q}_{\text{wall}}$ will be compensated by melting of the freeze lining or solidification of the bath material to attach to the freeze lining through $\dot{Q}_{\text{fusion}}$. Origins for such changes can be the presence of a phase with a high heat transfer coefficient, such as matte or metal or the freeze-lining detachment, which causes the thermal resistance of the wall to decrease. The latter is an important worst case scenario for the cooling system, because at that moment, it needs to extract both the extra heat input from the bath and the latent heat of fusion to reform the freeze lining [3].

Experimental Methods

The first application of freeze linings was found in an industrial context [15]. There are, however, a number of drawbacks (reduced safety due to explosion risk in the case of water leaks inside the furnace, high pumping costs, and high heat losses when the slag is severely superheated), but the majority of these issues can be tackled by improving the understanding of the behavior of the freeze lining inside the furnace. This requires a systematic investigation of the microstructure, composition, and heat transfer characteristics of freeze linings [34]. For this purpose, several experimental techniques can be used.

Cold Apparatus

The bath flow rates near the interface are important, but due to the complexity of pyrometallurgical reactors, it is difficult to use for example known empirical equations to calculate the convective coefficient. Direct measurements are, thus, necessary to determine h_{b} as a function of the various parameters. Such studies cannot be performed well in industrial reactors and are also difficult in laboratory-scale set-ups with normal pyrometallurgical bath compositions and temperatures. However, properly designed low-temperature model cells can be used [6]. In these cells, to make the model as similar as physically possible to real operations, model liquids are used, which have similar physical properties as the ones in the system they simulate. The dimensionless groups that are most relevant in solidification under natural convection are the Prandtl (Pr, ratio of momentum diffusivity to thermal diffusivity), Grashof

(Gr, ratio of the buoyancy to viscous force acting on a fluid), and Stefan (St, ratio of sensible heat to latent heat) numbers. The Rayleigh number (Ra) is the product of Pr and Gr [35]. The fundamental difference between low and high Prandtl number fluids is that the latter have hydrodynamic boundary layers that are much thicker than the thermal boundary layers [36].

Several small-scale, low-temperature models of furnaces have been made to analyze precipitation and solidification effects. Solheim and Thonstad [6] constructed a model cell, made of an aluminum plate, as a full-scale transverse section of an aluminum cell. The cell was designed to determine the effect of anodic gas evolution. Based on a comparison of physical properties of various liquids, molten biphenyl was chosen as the model liquid. To simulate anodic gas evolution air passed through openings distributed across the cell bottom. The heat flow through the frozen biphenyl layer was measured with thermocouples located on the copper sheet and in the freeze layer at a precisely fixed distance from the copper sheet. Most measurements were carried out with only one liquid phase (biphenyl). To investigate a second liquid phase (representing the metal) in the system, a liquid had to be chosen which was non-miscible with biphenyl, had an appropriate density, and was non-corrosive versus the cell material. Only a glycerol–water mixture met these requirements and was used in a few experiments, but severe experimental difficulties were encountered due to the evaporation of water and entrainment of biphenyl.

Banerjee and Irons [37] used mineral oil and an aqueous calcium chloride solution to simulate the slag and matte layers, respectively, in a 1/10-scale model of the Falconbridge ESF. In that study, precipitation in the matte phase was simulated. Robertson and Kang [30] experimentally studied the heat transfer and fluid flow in a slag-cleaning furnace, which works similar to an ESF. Eicosene wax was used to simulate molten slag, and a heated aluminum cylinder was used to represent the electrode. Eicosene wax has a melting point of 309 K (36 °C) and a Prandtl (Pr) number of 80, similar to fayalitic slags, but it does not allow for the formation of a two-phase zone.

The heat transfer at the cold solid wall is governed by the thickness of the hydrodynamic and thermal boundary layers, which depend strongly on the Pr number of the fluid [35]. Fayalitic slags that are used in nonferrous pyrometallurgy typically have Prandtl numbers between 50 and 150. Solidification in natural convection conditions has been studied in rectangular cavities that have opposing side walls maintained at different temperatures, with all other surfaces being adiabatic; this configuration is often referred to as a Bridgman cell. These studies have been performed for liquids with a low Prandtl number to understand the solidification of metallic alloys and other liquids such as water, with various Rayleigh numbers, Ra.

Guevara and Irons [35] used an acrylic glass cavity to study the freeze layer formation under natural convection conditions between two walls held at different temperatures. Polystyrene thermal insulation was used to insulate the top, front, back, and sidewalls. Two bath controllers were used to maintain constant temperature on each side of the cavity—cold on the left and hot on the right. Aluminum plates on each side were used to minimize the heat transfer resistance. Similar Grashof and Prandtl numbers for operating furnaces were obtained in the square cavity containing an aqueous solution of calcium chloride. The position of the solid front was tracked using a digital camera, and the temperature field was measured with thermocouples. The flow velocity field was measured using the two-dimensional particle image velocimetry technique. The temperature range was selected so that two phases would be present. Hence, 300 to 500 μm $CaCl_2$ particles were moving with the flow created by the natural convection. The particles were used as seeds for the Particle Image Velocimetry (PIV) measurement.

Pictures of the solid profile growth were recorded every 30 min, as shown in the left side of Fig. 1 [35]. The distinct interface was assumed to be at the solidus temperature. There is a clear difference in thickness in the upper and lower part of the freeze lining. This was caused by the larger heat transport in the upper than in the lower part of the cavity. The velocity measurements resulted in velocity field distributions, such as the one shown in the right side of Fig. 1. The $CaCl_2$ particles are moving with velocities that are at most 2 mm/s but, in the center of the cavity, are almost motionless. Guevara and Irons [35] assumed that for such small particles, the diffusion-controlled rates of heat and mass transfer are fast enough (of the order of a few seconds) that the thermal and chemical equilibrium are present at each location in the cavity.

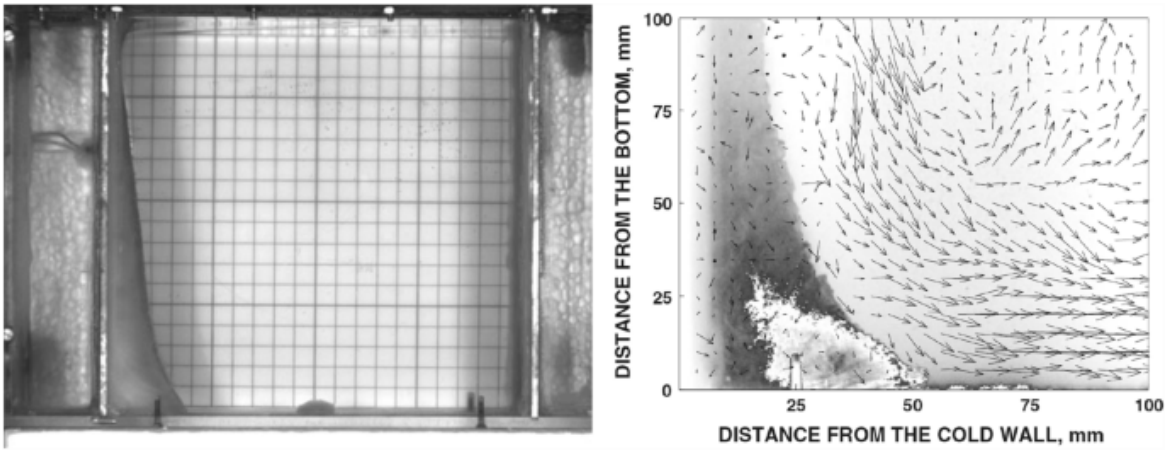

Fig. 1. Left: Example of freeze layer obtained on the cool side (left of the cell) of the cavity after 15 h. The operating conditions for this picture are $T_C = 25$ °C and $T_H = 45$ °C. Each grid cell is 10 × 10 mm; Right: Velocity field distribution after 15 h of solidification time at the bottom of the cell. The operating conditions for this picture are $T_C = 20$ °C and $T_H = 40$ °C. Reprinted with permission from [35]

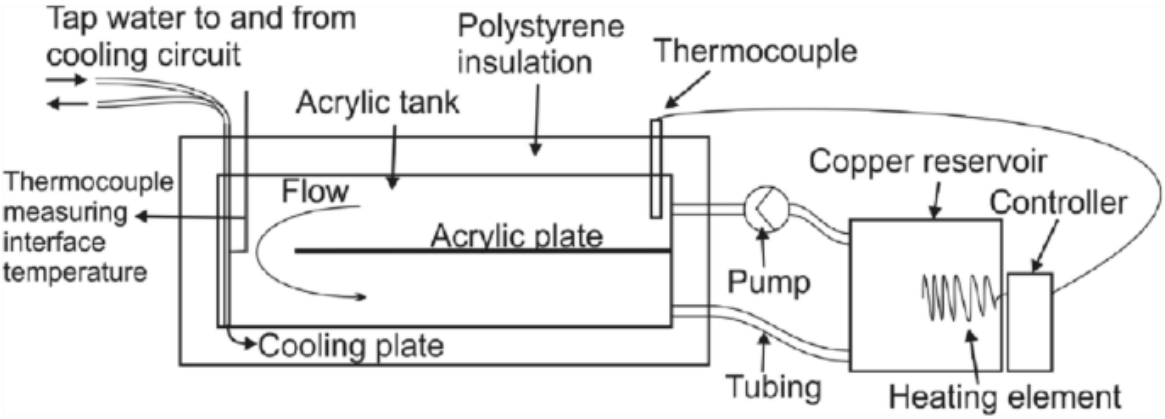

Fig. 2. Schematic of the experimental apparatus which also takes into account forced convection. Reprinted with permission from [32]

Crivits et al. [32] further optimized the apparatus, as shown in Fig. 2. They also used an aqueous solution with $CaCl_2$ in a transparent acrylic tank. The freeze lining forms on a water-cooled copper plate, and on the other side of the tank, the bulk solution was heated in a separate copper tank with a spiral-shaped titanium-heating element. The use of such a separate tank to heat the liquid significantly increased the time spent by the solution above its liquidus temperature. The improvement of the apparatus further consisted of using forced circulation

with a pump and directing the resulting flow to the surface of the copper plate, by positioning a thick acrylic plate in the middle of the tank, which left a 5 cm gap between the cooled copper circuit and the acrylic plate for the liquid to pass. Note that no detached crystals were observed within the liquid.

Cooled Probe Technique

Experimental techniques to study slag solidification include

- Controlled cooling in a furnace;
- Quenching in a cooling medium or on a cooled plate;
- Single hot thermocouple technique (SHTT);
- Double hot thermocouple technique (DHTT); and
- Confocal scanning laser microscopy (CSLM) with a high-temperature reaction cell.

They all control the cooling trajectory of the slag but clearly have their limitations: the temperature control happens on the whole system so that no temperature gradient can be imposed; some nonferrous slags contain iron oxide, which renders the slags non-transparent so that certain techniques are no longer useful. Furthermore, they typically investigate limited sample sizes, which may influence the cooling path (note that in reality, the lining is in contact with a large molten bath with an almost constant composition) [38].

These limitations do not apply to the cooled-probe technique, which can be used to create freeze linings under controlled conditions in a laboratory setting and to investigate the formed microstructure and its evolution [38]. First, the bath is molten in a furnace, after which the cooled probe is submerged in the molten liquid and the lining starts to solidify on it due to its cooling. The formed lining is quenched completely, after which microstructural and phase analyses are performed on the deposit [39].

The first mention of the investigation of the microstructural evolution with such a type of set-up was done, as far as the authors are aware, by Thonstad and Rolseth [7]. They did not use a cooled probe, but a cooled wall to investigate the formation of side ledge in cryolite. This was done in laboratory cell made from heat resistant steel. The cryolite melt was heated by passing an AC current between two steel rods dipped in the melt. All cell walls were insulated, except for one. A solid ledge would then only form at that cold wall. Thermocouples positioned within the cell wall enabled monitoring the heat flow through the ledge. The melt was stirred, and flow was directed along the vertical cold wall. The latter does not allow the study of heat transfer coefficients as this requires a well-defined flow pattern, which could not be established in this apparatus. First, the full bath was molten by also insulating the cold wall and the insulation was afterwards removed so that a ledge was formed on the cold wall. The phases present in the ledge and the bulk ledge composition were determined using X-ray diffraction, and X-ray fluorescence and wet chemical analysis, respectively.

Taylor and Welch [40] were the first to use a rotating internally cooled probe, made of graphite, in cryolite instead of a cooled wall. They observed that the ohmic heat production in the electrolyte under the anodes is six times higher than the heat in the system if the anodes were replaced by a vertical surface 10 °C hotter than the melt. Thus, the ohmic heat production results in much higher buoyancy forces, which cause much stronger natural convection than predicted for an isolated flat plate. The cylinder was immersed in molten cryolite superheated 4 to 8 °C above its freezing point. Their main focus for measurements was on the temperature

distribution throughout the electrolyte and the probe and also the growth of the solid deposit in its totality. Solheim and Støen [41] also used a probe, which was made from stainless steel and was air-cooled. The reason of the use of this probe was of a more practical nature: once the melt was sufficiently heated (5–15 °C above $T_{liquidus}$ of the bulk melt), the probe could be inserted, which was much more practical than working with a cooled wall. To compensate for the cooling of the melt by the probe, the furnace controller was set ± 15 °C higher. The actual microstructure was not analyzed either, but the samples of the deposit from different distances from the surface of the probe were taken for analysis by filing off the deposit.

Verscheure et al. [34] and Campforts et al. [38] further improved the apparatus by rotating the crucible which contained the liquid bath and wherein a cooled probe is submerged to form a solidified layer. In this way, the slag is not only subjected to a similar temperature gradient and cooling trajectory, but the fluid flow and its influence can also be investigated and make the apparatus closer related to the industrial system. Their apparatus is shown in Fig. 3. The crucible rotation enhances the temperature and compositional homogeneity of the bath through forced convection. The effects of the liquid flow rates on freeze-lining formation mechanisms (i.e., dislodging crystals and changing compositional and temperature gradients) are possible but have not been investigated [42].

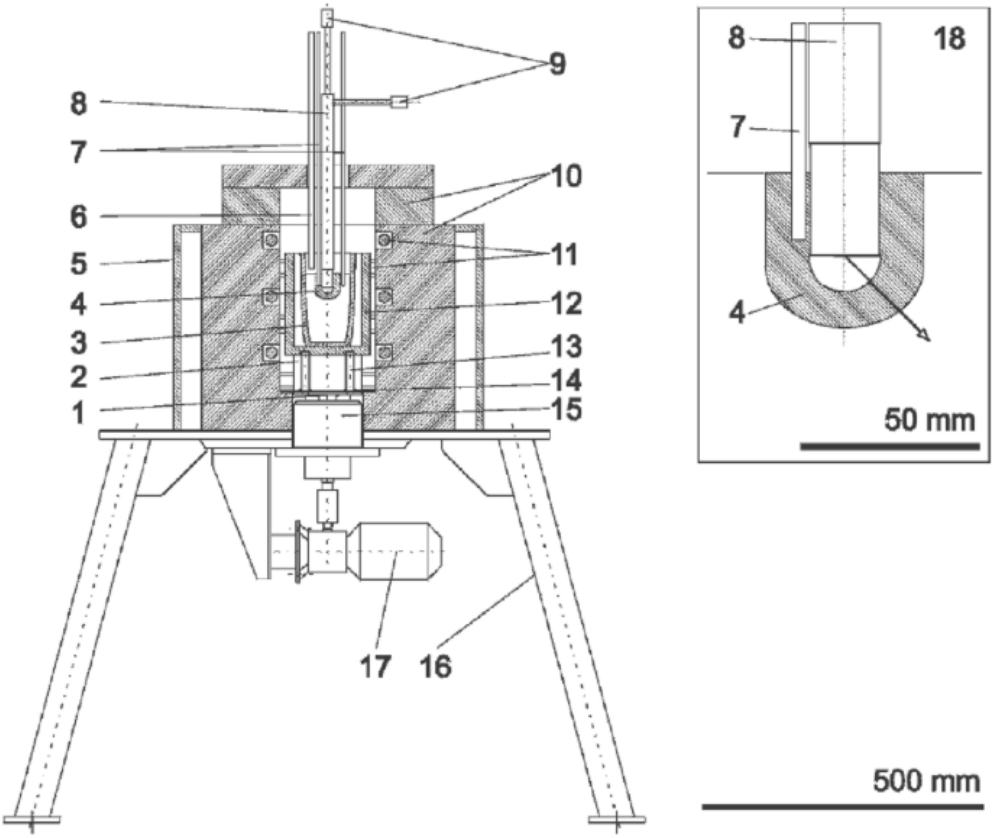

Fig. 3. Apparatus (1) rotary steel supporting disk, (2) refractory insulation disk, (3) slag-filled crucible, (4) solidified layer or freeze lining, (5) metal furnace covering, (6) shielding gas supply, (7) thermocouples for measurement of bath temperature and freeze lining temperature, (8) water-cooled probe, (9) location of water temperature thermocouples at connection of water piping, (10) furnace insulation, (11) silicon carbide-heating elements, (12) clay graphite crucible, (13) metal pin for fixation of the crucible rotation, (15) water-cooled guidance, (16) furnace support, and (17) electric motor. In (18), a detail of the freeze lining is shown and the location used for microprobe analysis is indicated with an arrow. Reprinted with permission from [34]

Furthermore, they changed the probe lay-out to two coaxial tubes so that a separate in- and outlet were present, to better control the flow. The water temperatures at in- and outlet could also be continuously monitored. Verscheure et al. [34] used a copper probe, whereas Campforts et al. [38] used a stainless steel probe. Furthermore, several thermocouples near the probe measured bath temperature as well as temperatures within the lining once it formed. The solidified layers can be analyzed afterwards with optical microscopy, electron microscopy, electron probe micro-analysis, and X-ray diffraction. When crystals are present, the order of crystal formation is determined by analyzing which crystals entrap others [43].

During the first experiments, it seemed that no perfect equilibrium was reached, because for long submergence times and low furnace powers, complete solidification of the bath was observed. The cooling by the probe was too strong compared to the heat input from the liquid slag bath. Using a less intensive cooling probe, such as a gas-cooled probe, was suggested to solve this [34, 38, 44]. This indeed solved the issue, and steady state was obtained [43].

A further addition to this type of apparatus was done at Aalto University [23], by automating part of the apparatus: there is an automatic system to remove the probe from the bath, yielding more consistent results, but possibly influencing the quenching speed.

The chosen type of crucible turned out to be particularly important, as could be expected as this is an important parameter in all pyrometallurgical experiments. For example, Jansson et al. [45] found that the experiments with industrial calcium ferrite slag were quite problematic. This was because the viscosity of the slag was low enough to allow slag leakage. They explained this by describing how during heating, some microcracks form in the crucible, which expand afterwards, due to the quick dissolution of magnesia into the molten slag.

In most experimental studies with the cooled-probe technique, focus was put on the freeze-lining formation kinetics and mechanisms with direct growth on a cooled metal surface of the probe. This is, however, only valid for part of the industrial freeze linings, because many designs have a brick layer between the molten bath and the cooler or the cooling elements have refractory bricks as part of the design. This is why, Kalliala et al. [46] covered the probe with a ceramic refractory-lining sleeve. The metal probe and refractory sleeve had different thermal expansion coefficients, this fact together with assembly-required tolerances, created an air gap, which dominated heat transfer. This modified the heat transfer circuit and increased the average temperature of the refractory, which in turn affected the slag's ability to stay molten in the open porosity of the refractory, allowing the slag to quickly infiltrate the pore system. The immersion time of the experiments was only 30 min, but this was sufficient for the molten slag to penetrate the open porosity of the refractory sleeve. The presence of the refractory sleeve clearly reduced the freeze-lining thickness. Furthermore, the microstructure of the lining was much more uniform throughout the layer.

Freeze-Lining Microstructure

For a freeze lining to be stable, the process material must form a solid layer on the reactor wall, but most importantly, this layer has to remain attached to the refractory wall. Ideally, this layer should not spall, but if it does, a new layer should form immediately. This behavior of the freeze lining depends on freeze layer formation and its thermal history, indications of which are found in the microstructure. The local microstructure of the freeze layer also determines its physical, mechanical, and chemical properties, and therefore, also its stability and performance [44, 47].

The microstructure of freeze linings has been studied for cryolite salts of the Hall–Héroult process [7, 41, 48], the Al_2O_3–CaO–SiO_2 slag system [49], zinc-fuming slags [10, 34, 50] synthetic lead slags [42, 43, 47], industrial lead slags [34, 44, 51, 52], and copper smelting and refining slags [23, 24, 29, 33, 39, 45, 53,54,55,56]. The reason why the local microstructure of the freeze lining is so important is best illustrated with an example: the microstructure will influence the melting of the freeze lining. For example, a glass phase with the same composition as the slag bath will melt more easily than large crystals of a phase with a different composition from the bath [44].

Zone Formation

Freeze-lining formation is typically investigated with a cooled-probe technique (cfr. Section 2.2) [44]. The solidified layers show a complex microstructure which depends on the distance from the probe. The solidification velocity and temperature gradient at the liquid/solid interface influence the solidification mechanism and, hence, the resulting microstructure [38]. This solidification rate and temperature gradient are continuously changing during the formation of the freeze lining, resulting in the formation of different zones: [44]

- a zone consisting of an amorphous matrix with small precipitates, positioned closest to the cooled probe and called ‘zone 1’;
- a zone with equiaxial crystals: ‘zone 2’;
- a zone with columnar crystals: ‘zone 3’;
- another zone consisting of an amorphous matrix with small precipitates, similar to the first one, called ‘zone 4’ and adjacent to the liquid bath.

To understand freeze-lining formation, the local temperature and its dependence on the distance to the probe should be considered. The slag at the cooled-probe side is cooled very rapidly to a low temperature due to its direct contact with the cooled probe; consequently, a glass phase is formed. This solidified slag layer then acts as an insulating layer on the probe. Thus, the temperature further away from the probe increases. Hence, the next slag layer solidifies more slowly and will be at a higher temperature in the end. The temperature as a function of the distance from the probe evolves such as shown schematically in Fig. 4 (black curves in graph) [44].

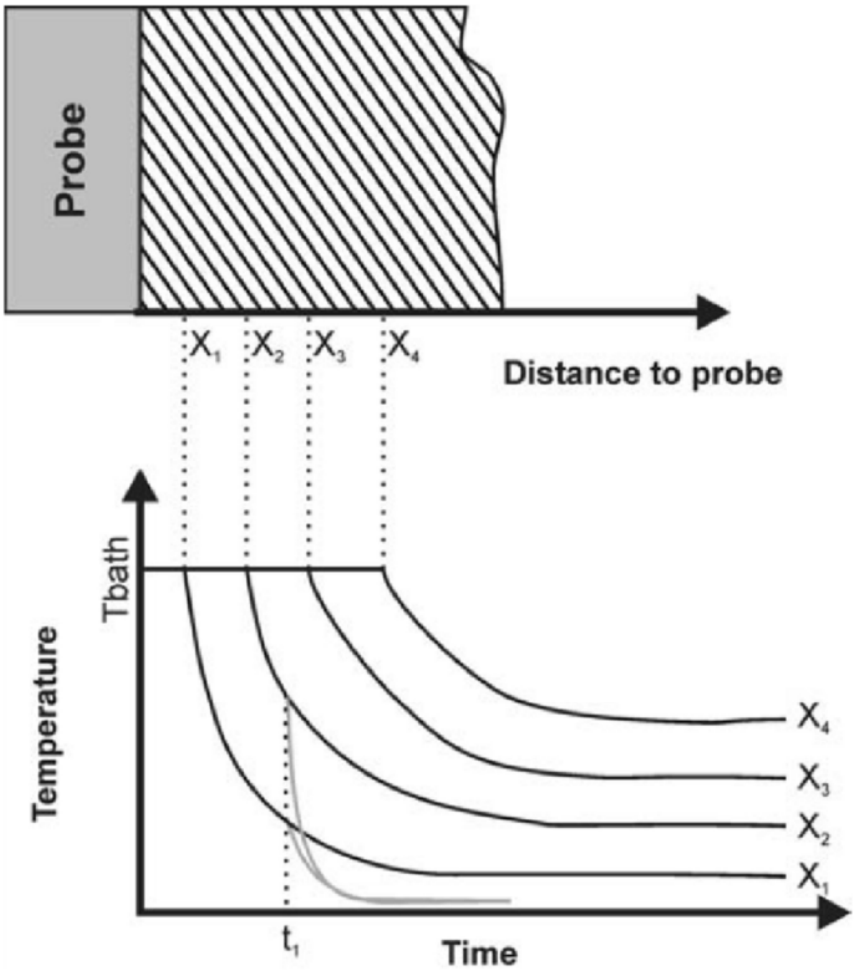

Fig. 4. Schematic drawing of temperature evolution in a freeze layer as a function of time for different distances (x_1 through x_4) to the probe surface. The black curves are the evolutions during the experiment, and the gray curves are the evolutions after removing the probe from the liquid bath at time t_1 and during cooling down to room temperature. Reprinted with permission from [44]

With the higher temperatures further away from the probe, the solidified slag is annealed as is shown for the larger submergence times, in Fig. 4. This means that, depending on the location, the microstructure in the freeze layer can coarsen further with time [44]. This was later verified by Jansson et al. [29]. The glassy structure clearly showed signs of crystallization. When the probe is removed from the bath, the freeze layer cools down fast to room temperature, as shown by the gray lines in Fig. 4, starting from time t_1. This cooling is assumed to have only a limited effect on the microstructure [44]. With the higher temperatures further away from the probe, crystal growth becomes possible, but this also depends on mass transport.

Mass Exchange and Reaction Kinetics

A distinction can be made between short-range mass transport, in which the local mass exchange between glass and crystals does not change the global composition of the freeze lining, and long-range mass transport, which is the mass exchange parallel to the heat flux and which results in a global change in the freeze-lining composition. In the layers closer to the probe and, thus, at lower temperatures (glass phase and glass with equiaxed crystals in it), it is assumed that only short-range mass transport occurs. In the columnar crystal layer, long-range

mass transport influences the growth. Note, however that not only the mass transport of the main components is important but also the mass transport of minor components can have a strong effect [51].

For certain short-duration experiments (15 min and less) [42], the glass phase close to the crystals was observed to be brighter than the glass further away from the crystals. Figure 5 shows these lighter (high PbO content) and darker (low PbO content) areas for the 5-min microstructure. These inhomogeneities illustrate the mass transport taking place in the system (mixing of PbO-rich liquid at the crystal–liquid interface with the bath liquid). This mixing is probably enhanced by the density differences between the PbO-rich and PbO-poor liquid. Clearly, material properties of the melt, such as the viscosity, also influence the microstructure that is formed [42, 44, 51].

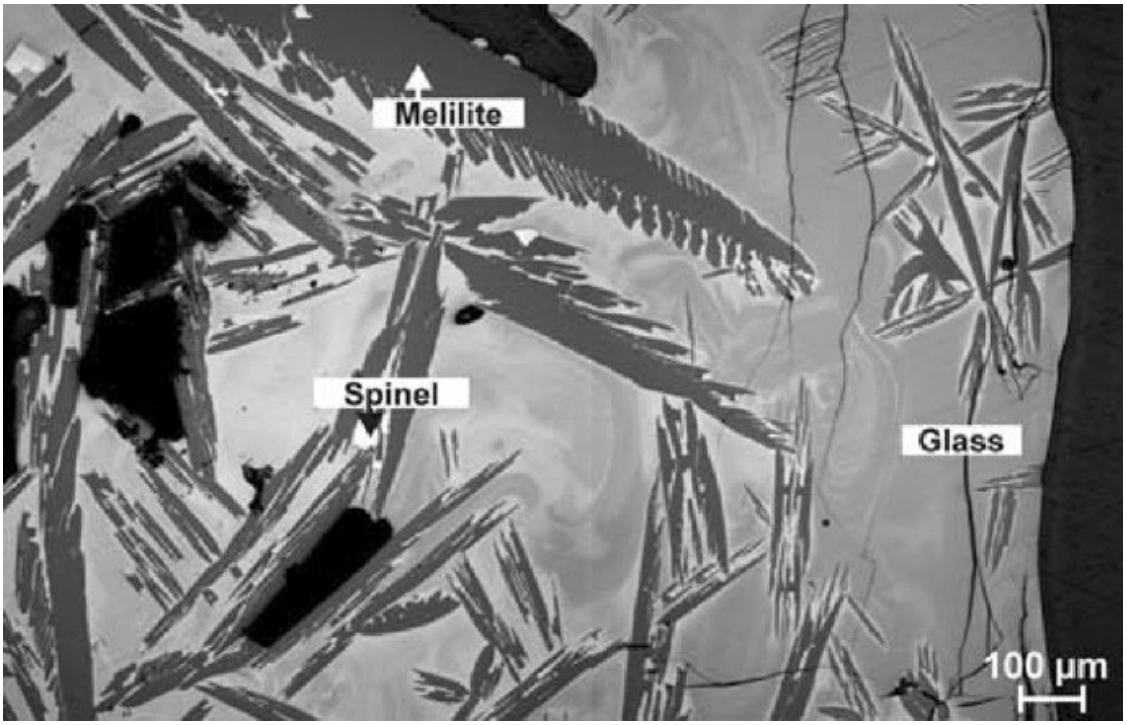

Fig. 5. Light optical microscope image of the 5-min freeze-lining microstructure taken at the bath–freeze-lining interface. The composition of the glass phase is not homogeneous. Reprinted with permission from [42]

The long-range mass exchange between the freeze lining and the bath determines the freeze-lining composition. However, the components not incorporated by the crystals have to be transported to the bath by diffusion or convection. The diffusion coefficient can be used to estimate the penetration depth and hence the impact of the diffusive transport [42]. Assuming 1-dimensional non-steady-state diffusion, the penetration depth is the distance at which the change in composition is at a certain value. This penetration depth can be found solving the Eq. (10):

$$\frac{c_{\text{surface}} - c_{\text{at -position } x}}{c_{\text{surface}} - c_{\text{original}}} = \operatorname{erfc}\left(\frac{x}{\sqrt{Dt}}\right) \tag{10}$$

where c is the concentration, x the distance from the surface, D the diffusion coefficient, and t the time. For slag systems, the diffusion coefficient of the most quickly diffusing ions at 1200 °C can be estimated at approximately 10^{-10} to 10^{-11} m^2/s [57]. Campforts et al. [42] calculated the penetration depths corresponding to these limiting values of the diffusion coefficient for a 1 and 5% composition change in 5 min time. The penetration depths for 1% composition change were 0.56 and 0.18 mm, respectively, and 0.43 and 0.14 mm, respectively, for a 5% change. They observed that the freeze lining grew 10 mm in the first 5 min. Therefore, they concluded that the solidification rate is most likely higher than the diffusion rate.

Furthermore, the impact of heat and mass transfer can be compared with the Lewis number (Le = the heat diffusivity/the diffusion coefficient). For the slag used by Campforts et al. [42], this was estimated to be 4×10^4. This very high value means that the mass transfer by diffusion is much slower than heat transfer. When the freeze-lining approaches its steady-state thickness, the effect of diffusion becomes more apparent.

Campforts et al. [42, 44] explained the changing crystal morphology and scale in the layers by the general solidification theory and the continuously changing solidification conditions. Two factors are important: the solidification rate (V) and the temperature gradient at the solid–liquid interface (G). The growth morphology is determined by the ratio of those two (G/V). For a high G/V, a planar front forms, and when G/V decreases, columnar crystals without any branches appear, followed by dendrites, and, finally for a low G/V, equiaxial crystals form. The scale of the microstructure is determined by the product $G \cdot V$. For a high value, fine grains are obtained and for low values coarse grains.

The formation of the four different zones can now be discussed in view of these two factors: [44]

- In zone 1, closest to the cooling probe, the liquid slag is rapidly quenched[Footnote 1] and is in almost direct contact with the hot bath. At the moment of submergence, the temperature is locally still very high, resulting in a low G/V ratio and a high $G \cdot V$ value. As a result, the microstructure consists of an amorphous phase with a limited fraction of small crystals, which forms during quenching. The composition of the freeze layer in this zone is the same as the bath composition. The crystal size can vary but does not depend on the submergence time. Thus, it is not due to annealing of the crystals, but perhaps due to less contact between the probe and the lining, so that the slag sometimes quenches less rapidly and slightly coarser crystals can form. Some of the larger particles can also be present from the liquid bath, if subliquidus temperatures are used.
- In zone 2, the temperatures are lower than in zone 1 at the moment of formation and, thus, produce a higher G/V and a lower $G \cdot V$ than in zone 1. Hence, equiaxial crystals form, which are bigger than in zone 1. In between the crystals, an amorphous matrix is present as well. No annealing effect is observed in this zone, either. The composition of this zone of the freeze lining is the same as the bath composition.
- In zone 3, G/V increases further, so that columnar crystals can form. But this means that not only heat transport but also mass transport controls the growth of the layer. If the solidification rate is similar or lower than the mass transport rate, concentration gradients can appear in the liquid at the solid–liquid interface. This can result in a locally higher liquidus temperature at the solid–liquid interface so that an area of constitutional undercooling forms, resulting in columnar growth. Furthermore, $G \cdot V$ decreases further resulting in larger columnar crystals. For larger submergence times,

the composition of the freeze layer in zone 3 differs slightly from the composition of the bath.
- In zone 4, a second amorphous matrix with small crystals is observed. This zone is liquid slag that sticks to the freeze layer during removal of the probe.

A higher bath temperature will result in a thinner freeze lining, solidification rates, and different temperature gradients, thus, affecting both the growth morphology and the scale of the microstructure. In the liquid bath, natural convection can be rather high due to the big temperature gradients present in the liquid bath. Introducing forced convection increases the convection in the bath and, hence, increases the heat convection and temperature and concentration gradients at the solid–liquid interface. The effect on the solidification rate is not clear, but experimental results [44] show that the freeze layer thickness is more or less constant with more mass transfer. The thickness of the zones and the microstructure types that form, however, change.

It is very interesting to note that Campforts et al. [44] observed that two microstructure types can be formed for similar experimental conditions. The two microstructure types were even observed within the same freeze layer. Hence, local variations, even within a single experiment, can result in the formation of the different microstructure types.

The interpretation of the microstructure evolution suggests that similar freeze-lining formation mechanisms occur for all slags [43]. In other systems, the solidified layers of the nonferrous slag show a different series of microstructures but are also formed through the same mechanisms [38]. However, it is noteworthy that some observations described above are not observed for the Hall–Héroult cell [7, 8]. In this case, the composition of the freeze layer will vary from the primary phase at low solidification rates to the bath composition at high rates. Contrary to the cryolite salt freeze lining, the composition of the slag freeze lining in an industrial nonferrous slags [34] is more or less constant for high to intermediate cooling rates, and equals the bath composition. However, still none of the microstructures consists of only the primary phase. This implies that the temperature of the freeze-lining surface for slags is lower than the liquidus temperature of the bath [38].

Furthermore, different growth mechanisms corresponding to different crystal structures also have implications, i.e., some crystals form a closed network of large broad crystals with a small amount of matrix in between the crystals, such as Melilite, whereas others form an open network of long thin crystals with a large amount of matrix in between the crystals, such as Olivine. In a closed network, the freeze layer must exchange components with the liquid slag bath to grow. In an open network, the solid layer can exchange components with the local matrix in between the crystals [51]. This influences the ability of a phase to interlock with the glass phase. The local conditions and the stability temperature range of the interlocking crystals are important for this interlocking ability [43].

Consequently, the number of layers was later extended to 7 to make the distinction between the different types of crystals (open versus closed). Their formation is illustrated in Fig. 6 and their description is summarized in Table 1 [43]. Note that not all layers are necessarily present in every system.

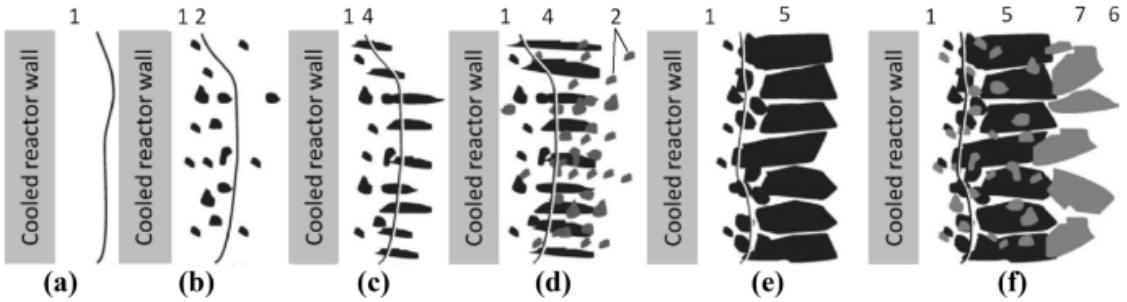

Fig. 6. Scheme of different stages in freeze-lining growth over time: **a** high viscosity glass layer (layer 1); **b** non-interlocking crystals in high viscosity glass layer (layers 1 and 2); **c** interlocking crystals in high viscosity layer (layers 1 and 4); **d** both interlocking crystals and non-interlocking crystals in liquid layer (layers 1, 2, and 4); **e** sealing crystal layer of interlocking phase (layers 1 and 5) and **f** high-melting phase layer formed (layers 1, 2, 4, 5, and 7). Adapted from [43]

Table 1. Details of different possible layers in freeze linings in slags. (Adapted from [43])

nr	Name	Microstructural characteristics
1	Glass layer	Only glass phase is observed
2	Glass-with-crystals layer	Equiaxed crystals are present in the glass phase
3	Crystalline layer	Slag is fully crystalline
4	First 'crystals-in-liquid layer'	Crystals are interlocked and contain liquid in between
5	Sealing-crystals layer	Large broad crystals that form a dense layer
6	Entrained-slag-bath layer	Similar to the glass layer but located at the bath side of the freeze lining
7	Second crystals-in-liquid layer	Crystals are interlocked and contain liquid in between

Note that not all layers are present in all formed freeze linings

Microstructure-Related Operational Demands

A freeze lining protects the reactor wall, when it restricts the contact of the corrosive liquid bath with the wall, but it should also remain stable during variable process conditions (composition and temperature). The bath temperature is typically close to or higher than the liquidus temperature and often much higher than the glass transition temperature (which can be estimated at roughly 2/3 of the absolute liquidus temperature). Because the freeze-lining thickness increases with a higher bath-lining interface temperature (but still below the liquidus temperature), a better protecting freeze lining can be obtained not only if the interface temperature is closer to the bath temperature, but also if the shrinking of the freeze lining does not solely depend on a temperature change [43].

These prerequisites make it possible to decide whether the stable layer should consist of glass or crystals [43]:

- A glass layer grows according to the temperature distribution in the process material at the reactor wall. This means that such a freeze lining will easily disappear at increasing temperature.
- A layer at the interface containing large crystals does not only depend on the temperature distribution. The crystals are in equilibrium with the bath in a temperature range around the targeted bath temperature (the larger this range, the better), and their

composition differs from the bath composition. This different composition can slow down the shrinking of the freeze lining because the crystals have to dissolve in the bath, which requires mass transfer.

Campforts et al. [42, 43] proposed the following operational demands for a protective freeze lining: rapid formation and a sufficient stability with respect to changing heat input and bath composition. They concluded that these demands can be fulfilled with the growth of an initial layer dominated by the presence of interlocking crystals in combination with the subsequent formation of a high-melting crystalline layer at the bath–freeze-lining interface. The latter should be in equilibrium with the slag bath, and its composition should differ sufficiently from the bath composition [43]. The high-melting phases protect the refractory from corrosion, while the low-melting phases attach the high-melting phases to the refractory [58].

The formation of requested high-melting crystalline layer may take a certain time, because mass exchange is required. However, this mass exchange also provides the freeze lining's higher stability in the long run. Regarding the type of crystals, interlocking crystals have to be distinguished from crystalline phases forming only separate crystals. Interlocking crystals will stabilize a freeze-lining layer by the formation of a crystals-in-liquid layer, as opposed to the separate crystals. The interlocking crystals should be stable at sufficiently high temperatures, but the actual protection comes from the high-melting crystals, which are formed later on, as illustrated in Fig. 6 [43]. Note that the interlocking crystals should not necessarily consist of the primary phase of the slag system. Thus, by slag engineering, the phases of which the freeze lining is constituted can be optimized to obtain rapid freeze-lining formation. [42] Slag engineering changes slag properties such as viscosity, but also the type of crystalline phases, the temperature range in which it is stable and the crystallization behaviour. With these changes, the freeze-lining formation rate and its stability can be influenced. However, in reality not only the freeze-lining presence is important. The process conditions should also remain optimal, resulting in a certain process window that needs to be aimed at. Furthermore, it is important to note that slag engineering might not always be possible. For example, in ilmenite smelting, additions to the slag are unwanted, because the slag is the final product [43].

Macroscopic Freeze-Lining Formation Mechanism

Thermal-Based Mechanism

Freeze linings result from a thermal balance between heat transfer from the bath to the lining and heat transfer through the lining. Thermal disturbances could result from an incorrect power input for the considered feed rates and compositional disturbances result from an incorrect amount of input of a certain reactant [59]. Because of the importance of heat transfer, the first proposed mechanism is mostly focused on this aspect.

For the thermal balance, the interfacial temperature is a particularly important parameter. However, in most literature data, the interface temperature between the bath and the freeze lining was assumed to be the liquidus temperature. For example, for heat conductivity measurements, Warczok and Utigard [4] assumed that the temperature at the solid/liquid interface was constant and equal to the liquidus temperature of the slag, also most of the early models considering freeze lining (see Sect. 5) consider the interface temperature to be equal to the liquidus temperature.

This assumption comes from the following reasoning: in periods without thermal balance, the heat flux from bath to the lining is different from the heat flux into the lining and that difference is used for melting or freezing until the thermodynamic instability is resolved. Furthermore, if the crystal phases are already present, there is no nucleation barrier. This means that the attachment of atoms to the deposit occurs easily. If the deposit would grow or melt, this would require mass exchange, because the chemical composition of the lining is different from the bath. However, as no net movement of the interface is observed at steady state, there is no net thermodynamic driving force for crystal growth at this boundary. Consequently, the steady-state condition translates to thermal and chemical equilibrium. Hence, the solid primary phase at the interface is in chemical and thermal equilibrium with the bulk liquid at the liquidus temperature [9, 31, 38, 41].

From this assumption, it is expected that there is a primary-phase-sealing layer at steady-state conditions [54]. At steady-state conditions, the temperature profile remains unchanged with time, and the stagnant deposit thickness remains constant [60]. Because there is no nucleation barrier to overcome at the stationary deposit, the heat is continuously removed and there is a continuous supply of fresh chemicals from the bulk bath to the interface by relatively fast mass transfer, the crystallization on the outer surface will continue until equilibrium is reached at liquidus temperature of the bulk bath (T_{liquidus}). So that the final phase formed is assumed to be the primary phase [54].

Thermal, Chemical, and Flow-Based Mechanism

However, recent experiments [38, 39, 42, 44, 47, 51, 54] observed that the interface did not only consist of the primary phase. Note that the presence of the primary phase was observed, but not as a single phase, which was expected based on the previously assumed mechanisms [54].

This set of recent experiments also found interface temperatures varying between the solidus and liquidus temperature. In these investigations, laboratory-scale freeze linings were produced with the cooled-probe technique (cfr. Section 2.2). The temperature evolution is usually measured in this kind of experiments with thermocouples, from which the full thermal profile across deposit is determined with interpolation in between temperatures measured. Initially, the thermocouples were fixed at a certain distance from the probe, but later, Crivits et al. [56] determined the positions of the thermocouples after the experiment by cutting the freeze lining perpendicular to the probe at the positions of the thermocouple tips and measuring the distances from the probe. On top of that, the temperature profile has also been estimated using the experimentally determined position and composition of the phases, in combination with the phase assemblages predicted with thermodynamic software, such as FactSage.

One could suggest that perhaps, steady state is not yet reached in these experiments, but this was always checked. For example, Fig. 7 clearly illustrates that steady state is reached (left part of the figure), but that the interface (indicated with ‘stationary deposit,’ between layers 4 and 4’ at temperature T_f) has a temperature lower than the liquidus temperature.

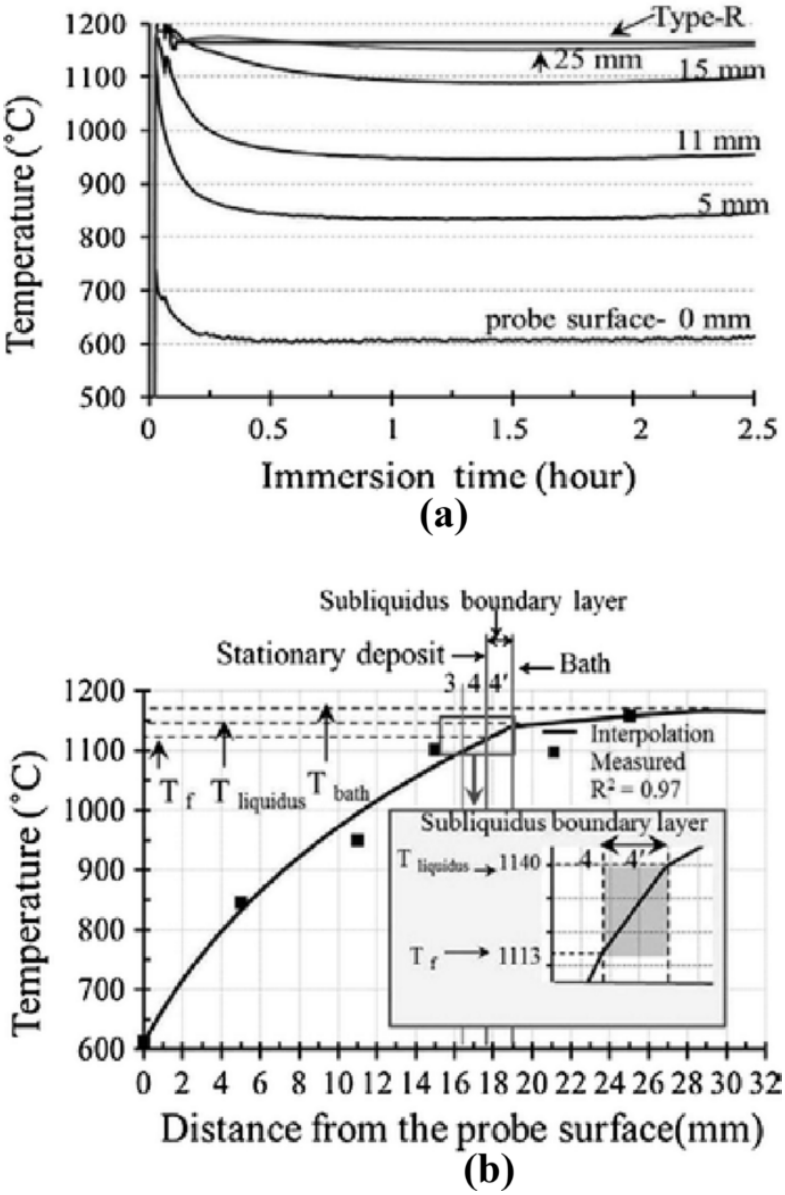

Fig. 7. a Temperature vs immersion time at positions across the freeze-lining deposit and bath. **b** Temperature distribution across the deposit and bath at steady-state conditions; T_f = the interface temperature; T_{bath} = 1438 K (1165 °C), air flow rate: 100 L/min speed of rotation: 20 RPM (0.05 m/s, for steady-state thickness), and immersion time: 2.5 h. Reprinted with permission from [54]

Furthermore, Campforts et al. [47] observed that the heat transfer was relatively fast so that the steady-state temperature profile is reached quickly. The growth of the freeze lining was, on the contrary, slower. This is probably because the crystals form in undercooled liquid and not immediately after becoming thermodynamically stable. Hence, this also shows that assuming that the interface temperature is equal to the liquidus temperature will overestimate the growth rate of the freeze lining.

The question that remained was 'why does the freeze-lining not continue to grow until a solid layer of primary-phase crystals forms, the bath/deposit interface reaches the liquidus temperature, and chemical and thermal equilibrium with the bulk liquid is established?' [54].

With all the above-mentioned observations kept in mind, Fallah-Mehrjardi et al. [54] proposed a significant change in the mechanism and behavior of the systems to answer this question. They proposed that the steady-state thickness of freeze linings results from a state of dynamic equilibrium, rather than from thermodynamic equilibrium freezing. The relative rates of heat and mass transfer are important, as well as the speed of crystallization at that position. These processes occur close to and at the deposit interface. This proposed mechanism is generic and is applicable to all systems, not limited by certain compositional ranges.

Subliquidus Boundary Layer

Furthermore, the concept of a subliquidus boundary layer (Fig. 8) was proposed by Fallah-Mehrjardi et al. [54] for systems with relatively low mass transfer rates. This layer consists of detached crystals in liquid and both partial crystallization/remelting and continuous removal of solids take place in the layer. At steady state, there is a dynamic equilibrium between solidification of material on crystals moving towards the freeze lining and melting of material moving away from the freeze lining.

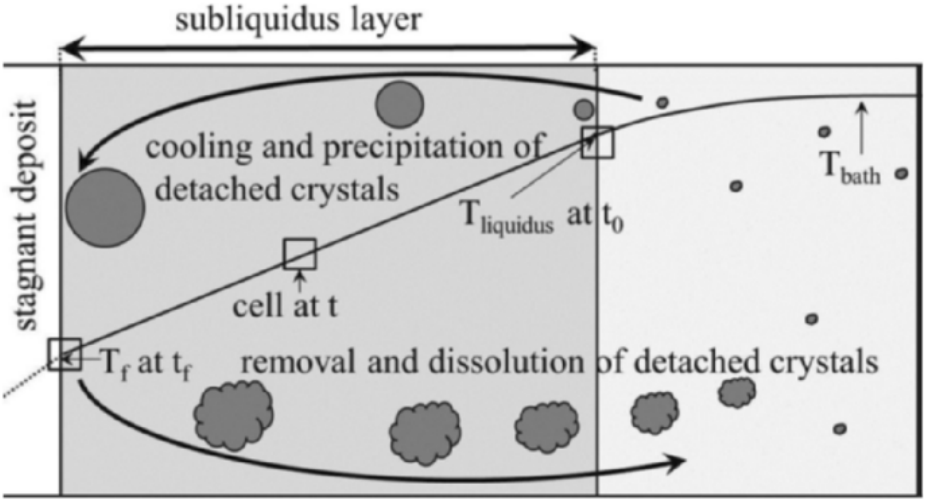

Fig. 8. Schematic of the conceptual dynamic steady-state framework for freeze-lining formation. Reprinted with permission from [60]

Due to convection (either natural or forced), 'fresh' liquid is delivered towards the stationary deposit. During its approach, the temperature gets lower from T_{bath} to T_{liq} without any crystallization taking place. Once the liquid portion crosses the point at $T_{liquidus}$, nucleation and precipitation of the primary phase start. Due to this crystallization, the composition of the remaining liquid also changes [54].

If the flow towards the stationary deposit is rather slow, there will be a local equilibrium between this primary phase and the surrounding liquid (and other phases), and this equilibrium will be preserved during the passage across the subliquidus boundary layer by short-range diffusion in the portion of liquid. It is common in various slags that the precipitation of several phases leaves a surrounding liquid that is high in silica content and hence has a higher viscosity. Furthermore, the presence of solids or their precipitation will increase the effective viscosity. This will further decrease the convective flow. When the liquid then arrives at the interface, there is no thermodynamic driving force to form the primary phase, either as fresh precipitates on the deposit or by cementing the precipitated primary-phase crystals from the liquid to the

deposit. Hence, the primary-phase crystals do not attach to the surface of the stationary deposit [54].

As mass transfer at interfaces results in the formation of turbulent eddy currents or flow cells, both the flow towards the interface and the flow away from it are present. Hence, the flow towards the interface brings the crystals to the interface, but the other part of the flow current also transports part of the liquid with precipitated crystals back to the bulk liquid. Due to the increasing temperature (also above T_{liquidus}), the returning crystals will redissolve into the bulk liquid [54].

Classification of Freeze Linings

The proposed mechanism can now be applied to several systems to explain the variety in observed interface temperatures and the different types of interface structure (with the absence or presence of a primary-phase-sealing layer at steady state) in freeze-lining research: [31, 54]

- $T_f > T_{\text{liquidus}}$: This situation corresponds to a traditional hot-face refractory design. In this case, high-melting components from the refractory are in direct contact with the liquid bath or can form solid phases with higher concentrations of these high-melting elements which are, thus, more stable compared to the equilibrium primary phase of the bath materials. However, continuous mass transfer from the refractory and slow dissolution and erosion may continuously consume the refractory. But still, this process may be slow and might guarantee furnace integrity for extended periods of time.
- $T_f = T_{\text{liquidus}}$: If relatively fast mass transfer from the bulk to the interface occurs, the primary-phase crystals can form a stable primary-phase-sealing layer with an interface temperature equal to the liquidus temperature. The essential high mass transfer rate could be achieved in systems with 'fluid' liquids or with intensive bath convection.
- $T_g < T_f < T_{\text{liquidus}}$: This situation results in the formation of a subliquidus layer and hence, as explained above, continuous crystallization towards the interface, without attachment, and redissolution back to the bath take place. However, there is no net growth of the lining. This results in the interface temperature being lower than the liquidus of the bulk bath. Systems with relatively low mass transfer rates, typical in liquids with higher viscosities or less agitated baths, will give rise to this condition. The microstructure of the interface layer can be open or closed with respect to mass exchange with the liquid bath, as also explained in Sect. 3.1 focusing on the microstructure.
- $T_f < T_g$: Systems with high glass transition temperatures and slow crystallization kinetics may result in an interface temperature lower than the glass transition temperature. The interface layer is in that case of the glass or microcrystalline type.

The proposed mechanism, thus, not only takes into account the thermal balances within the system, but also chemical equilibrium, slag properties (viscosity, thermal and mass diffusivity, nucleation and crystallization kinetics, liquidus shape of phase equilibrium, and dissolution kinetics) as well as the convective flow in the bath [54]. Note that, as mentioned by Crivits et al. [32], the rate limiting step can, in theory, be determined from the concentration and temperature profiles near the reaction interface. The existence of the subliquidus layer and taking into account various possibilities, would result in the set of layers as suggested by Crivits et al. [53], which is summarized in Table 2. Note that originally the subliquidus layer was annotated as number 4' by Fallah-Mehrjardi et al. [54], and the sealing layer was stated to consist only of primary phase. The categories proposed by Crivits et al. [53] take into account

that after extensive exposure, such as expected in industrial applications, the open crystalline layer may evolve into a sealed crystalline layer.

Table 2. Details of different layers in freeze linings in slags [53, 54]

nr	Name	Microstructural characteristics	Formation aspects
1	Quenched layer	Only glass phase (uniform and identical to bulk liquid)	High initial cooling rate remains below T_g
2	Devitrified quenched layer	Fine-precipitated crystalline solids in matrix of glass phase	Initially formed as glass, fine crystallites precipitated later
3	Closed crystalline layer	Mostly crystalline solids with residual liquid between crystals; Crystal dimensions increase further away from cold probe	Crystals precipitated directly from liquid, which was above T_g; no exchange of material with bulk liquid
4	Open crystalline layer	Large, widely spaced crystals with significant amount of liquid within open liquid channels	Open channels facilitate mass transfer with bulk liquid; liquid composition varies with distance from interface
5	Sealing layer	Consists solely of primary-phase crystals or other phases that are stable at the interface temperature	Theoretically formed at steady-state and chemical equilibrium
6	Subliquidus boundary layer	Intermediate layer between stagnant deposit and liquid bath	Temperature below $T_{liquidus}$ so that phases can precipitate
7	Entrained bulk bath liquid	Similar to the glass layer but located at the bath side of the freeze lining	Quenched after experiment, when probe is removed from bath

A final remark is given regarding typical calculations of heat flow rates using the assumption that the interface temperature was the liquidus temperature. This means that the effective superheats were greater than anticipated and reported, so that Fallah-Mehrjardi et al. [31] recommended that convective heat transfer coefficients of the bath at the interface (h_{bath}) should be recalculated. These values can also influence mathematical modeling of heat flow rates at the interface. If the heat flow rate is calculated from the heat transfer through the bath to interface, then the heat transfer rate will be underestimated because ($T_{bath} - T_f$) will be larger than assumed. If the heat transfer rate is based on the conductivity through the lining, the heat flow rate may be overestimated because ($T_f - T_{coolant}$) will be lower than assumed. For industrial design purposes, the maximum heat flow rate through the bath to interface and, thus, also through the wall and freeze lining is obtained when $T_f = T_{solidus}$.

Proof of Boundary Layer

Proof of the presence of this boundary layer can be found in several ways. It was already observed by Guevara and Irons [35] in a low-temperature physical model system (H_2O–$CaCl_2$). At steady state, they showed the presence of particles, 300 to 500 µm in diameter, of the primary phase circulating between the stable deposit interface and the superheated bulk liquid. They even used these particles to track the fluid flow in the system with PIV measurements, as shown in Fig. 1 [35]. They also estimated the times to reach thermal and chemical equilibrium in the particles to be small relative to the residence time in the subliquidus boundary layer. They observed the interface temperature to be equal to the solidus temperature, not the liquidus. This is a limiting case, of the presence of a subliquidus boundary layer with the interface being at the solidus temperature. For a low-viscosity and relatively fast flow, all small crystals will be carried away, and only material that solidified directly on the wall will remain. This results in $T_f = T_{solidus}$. This means that equilibrium crystallization takes place across the boundary layer [31]. The PIV measurements also showed the presence of flow cells, which once more supports the proposed mechanism [60].

Crivits et al. [32] used a very similar, but slightly different apparatus (cfr. Section 2.1), and reported some new observations: the formation of a 2-phase area within the deposit and the lack of any detached crystals in the bulk liquid, even at temperatures below the liquidus

temperature. Hence, the assumption of equilibrium solidification (as previously stated by Guevara and Irons [35] in the case of natural convection) is not valid in the forced convection system. Furthermore, they found that the steady-state interface temperature and deposit thickness depended on the phase that was in direct contact with the liquid bath.

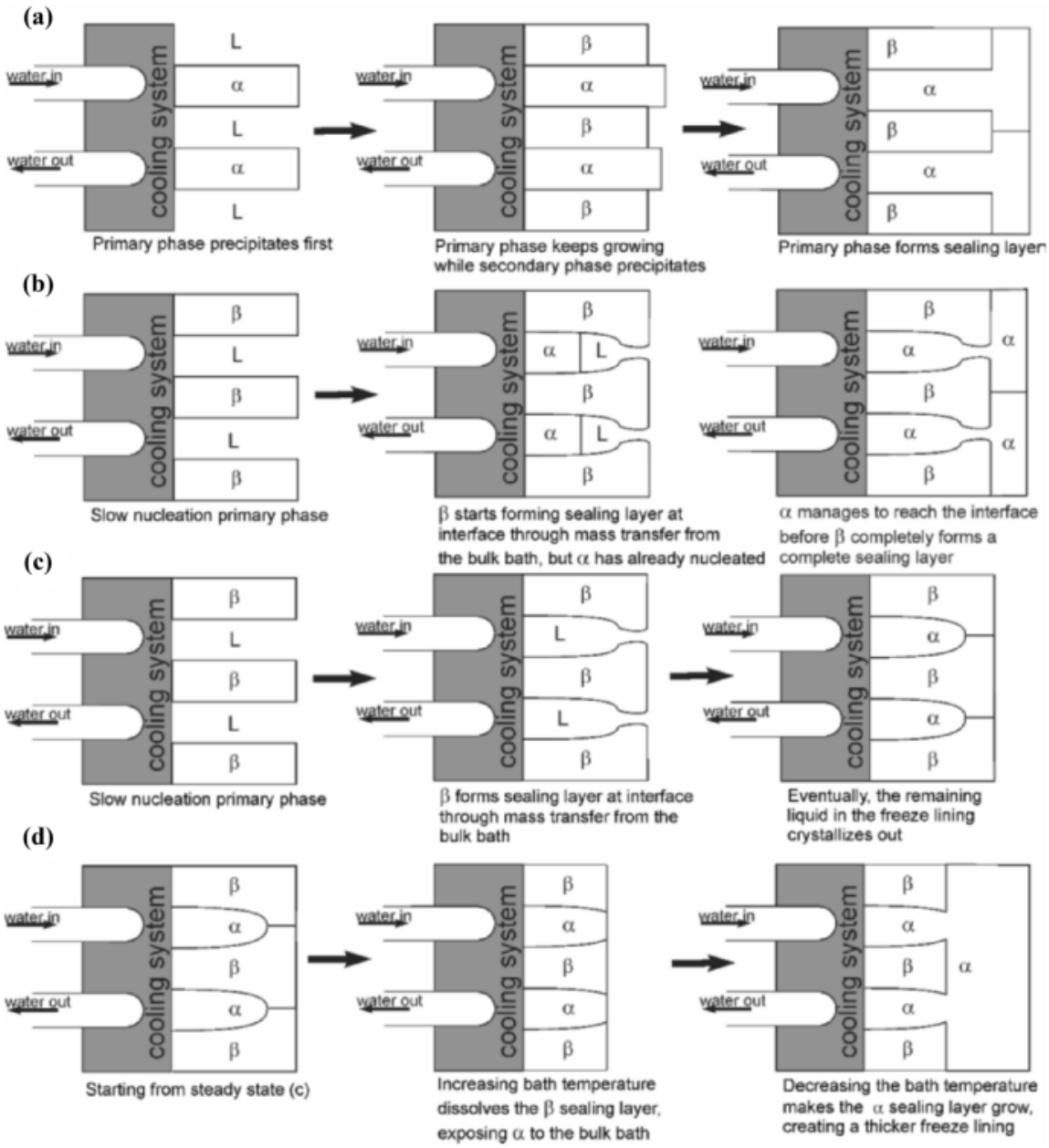

Fig. 9. Hypothesized microstructural changes during freeze-lining formation. **a** Expected growth of the freeze lining, with the primary phase α precipitating first; **b** The formation of the primary α phase is slow, resulting in the partial closure of the β layer at the interface; **c** Dynamic steady-state model where the formation of the primary α phase is inhibited. As a result, the secondary β phase forms a sealing layer; **d** Evolution of the freeze lining formed in (**c**) after an increase and subsequent decrease in bath temperature. Reprinted with permission from [32]

This can be explained by the dynamic steady state proposed by Fallah-Mehrjardi et al. [54], as illustrated in Fig. 9. For example, if the growth kinetics of the secondary β phase are such that it precipitates first and the subsequent nucleation/growth of the primary α phase is slow in comparison to the mass transfer, the secondary β phase forms a sealing crystal layer before the primary α phase reaches the interface. With no primary phase at the interface, the freeze lining stops growing when the interface temperature equals the temperature at which the secondary phase becomes stable. Moreover, any primary-phase crystals that do form in the liquid next to the interface due to the subliquidus temperatures circulate back to then dissolve into the bath. Guevara and Irons [35] observed solid crystals in the bath, because the crystals were only shortly present in the area with a super-liquidus temperature.

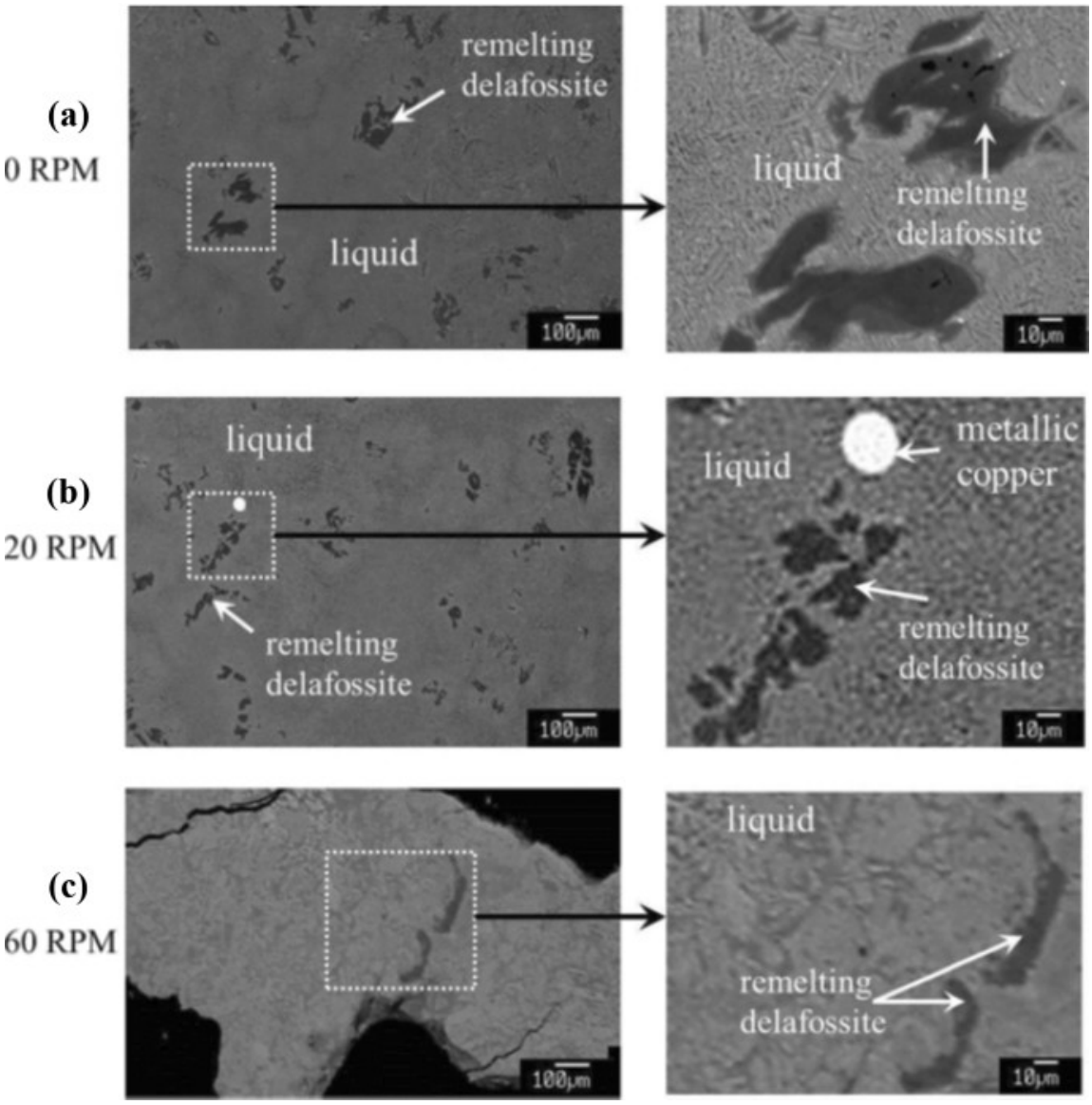

Fig. 10. Backscattered electron micrographs of bath samples taken after freeze-lining experiments at steady-state conditions. Cu–Fe–Si–Al–O system (15 wt pct SiO_2), bath temperature: 1438 K (1165 °C), air flow rate: 100 L/min **a** speed of rotation: 0 RPM and immersion time: 9 h, **b** speed of rotation: 20 RPM and immersion time: 9 h, **c** speed of rotation: 60 RPM and immersion time: 2 h. Adapted from [60]

Furthermore, in high-temperature experiments, after cooling the cold finger rapidly, the subliquidus layer was quenched and examined microscopically [54]. The subliquidus layer contained fine 'quench crystals' in a matrix of residual silicate glass that formed on not only rapid cooling after the experiment but also relatively large, 10–50 μm, primary-phase crystals. This large size and the observed morphology indicate that the crystals were also present in the melt at high temperature before quenching. Moreover, also detached and redissolving crystals in liquid slags [52, 60] were observed, as shown in Fig. 10. These particles had compositional gradients surrounding them, which indicate the mass transfer limitation of the dissolution of the particles.

Influence of Viscosity

The proposed mechanism was also verified with additional experiments, as it would be expected that the interface type and temperature can be changed by changing the system properties (chemistry or agitation). For example, the primary-phase-sealing layer is expected when the interface temperature is equal to $T_{liquidus}$, which happens if mass transfer across the boundary layer to the interface is faster than crystallization. This would be the case in low viscosity melts [54].

To verify this, Fallah-Mehrjardi et al. [54] compared a slag containing approximately 15 wt% SiO_2 to a slag with a lower amount (9 wt% SiO_2). Because the silica content of slags greatly influences its viscosity, the latter slag will have a lower viscosity than the former. The detailed temperature measurements showed that the freeze lining in the lower viscosity system reached a steady-state thickness after a shorter time. Furthermore, the microstructure of the deposit clearly contained a dense-sealing layer consisting of the primary phase (layer 5), and the interface temperature was the liquidus temperature of the bath. The presence of the primary phase at the interface indicates that there was indeed no nucleation barrier to the crystallization of the primary phase on the existing solid-phase surfaces. On the contrary, an open structure with a low solid fraction is formed in the higher silica slag, and the interface temperature is lower in the more viscous slag [60].

In another study, Fallah-Mehrjardi et al. [23] also investigated a non-silicate-based industrial calcium ferrite slag, with a much lower silica concentration (approximately 1 wt% SiO_2), known for their much higher fluidity. The observed layers showed a direct result from that: the glass layer (layer 1) and the open crystalline layer (layer 4) were not observed. They did observe a subliquidus boundary layer (6). The subliquidus layer contained several relatively large, detached crystals of the primary phase, and the proportion of the solids increased closer to the stagnant deposit. Hence, the interface temperature is below $T_{liquidus}$. The sealing layer consisted primarily of the primary phase, which they classified as a 'layer 5.' However, as this was not the only phase, we would opt to classify this as layer 3 (closed crystalline layer). They also briefly mentioned the sulfates that formed in the layer closest to the cooled probe.

This was further investigated by Jansson et al. [45]. They found that fine crystallites of calcium sulfate formed in the layer next to the probe. These sulfates can form directly from the slag and are known to have a low strength, which results in a poor stability of the formed freeze lining. The formed freeze linings are, thus, sensitive to spalling and descaling from the sidewalls of the converter. In the same investigation by Jansson et al. [45], a peculiarity of the macrostructure of the freeze lining was noted: it was 'very complex and not at all smooth as in the silicate slags.' Large dendrites and tetrahedra made up the lining and pointed towards the hot face. This indicated the direction of the thermal gradient and the heat flow in the lining.

More recent investigations in the 'Cu_2O'–'Fe_2O_3'–MgO–SiO_2 system [56] also observed a non-planar interface, even though the silica content was as high as 17 wt%. Crystals protruded from the freeze lining, and it was even observed that during the removal of the probe from the bath, at the end of the experiment, low-viscosity liquid slag drained from in between these crystals and returned to the bath. This non-planarity is an interesting observation because thermal steady state (with a constant freeze-lining thickness) is generally assumed to result in a planar interface. This is assumed because in the accepted solidification theory, as an interface is approached, the growth rate goes towards zero.

Crivits et al. [53] also measured the interface temperatures in CuO_x–FeO_y–MgO–SiO_2 system at copper metal saturation. The interface temperature was found to lie within uncertainty of the formation temperature of a solid compound. They hypothesized the following explanation: the formation of a compound is accompanied by a sudden change in chemical and physical parameters. Different solid compounds, hence, have a different nucleation rate, crystallization rate, and mass transfer and certain compounds are, thus, more likely to be deposited on the freeze lining, while others more likely continuously form and dissolve in the subliquidus layer, or do not form.

In another study [49], they investigated the Al_2O_3–CaO–SiO_2 system, which is relevant for, e.g., the iron blast furnace, but which seemed to have been neglected by freeze-lining research until then. The system and the phase equilibria within, however, are well investigated, so that Crivits et al. [49] seized this opportunity to investigate the influence of the composition (high and low SiO_2 region) on the freeze lining. In this way, they varied the viscosity of the slag (from very high, i.e., approximately 39 wt% SiO_2, to low, i.e., approximately 10 wt% SiO_2). They selected a wide range of compositions in different primary-phase fields of congruently melting compounds, having a similar liquidus temperature, liquidus shape (i.e., decrease in liquidus temperature as a function of composition on the crystallization path). Furthermore, no bulk stirring was applied and then mass transfer only happened through diffusion and natural convection. They found that all samples contained the primary phase at the interface and that the interface temperatures ranged from the solidus to the liquidus temperature depending on the composition. When comparing experiments performed in the same primary-phase field, they found that low-viscosity slags resulted in an interface temperature below the liquidus temperature and that high-viscosity slags had an interface temperature equal to the liquidus, which was in contrast with the previous findings of Fallah-Mehrjardi et al. [54], showing that a decreasing viscosity resulted in an interface temperature closer to the liquidus temperature.

Crivits et al. [49], hence, tried to explain their results as well as the results from Fallah-Mehrjardi et al. [54] that also considered slags with intermediate viscosities (approximately 15 wt% SiO_2) and low viscosities (approximately 9 wt% SiO_2). They explained all these results with the mechanism proposed by Fallah-Mehrjardi et al. [54] in combination with the inverse dependence of the mass diffusivity on the viscosity:

- In very viscous systems, mass diffusion to the crystals in the subliquidus region is slow, so that no local equilibrium is achieved in this layer and the freeze lining grows further.
- In systems with intermediate viscosities, mass diffusion towards the crystals within the boundary layer might be sufficient to achieve local equilibrium, resulting in the dynamic steady state with crystals being formed and redissolving in the boundary layer but not resulting in net change of the freeze-lining thickness.
- In low-viscosity systems, the thickness of the subliquidus boundary layer might become too thin, so that the timeframe for the crystals to nucleate or grow is too small so that

local equilibrium cannot be achieved again, resulting in further growth of the freeze lining.

The main difference of the investigated linings in the Al_2O_3–CaO–SiO_2 system [49] with previous freeze-lining research was the presence of a relatively large number of pores. It is proposed that these originate from the presence of dissolved species in the slag, of which the solubility decreases, when the temperature increases. Hence, gas bubbles are formed, which then get trapped in between the crystals of the freeze lining. The pores could have a large influence on the apparent thermal conductivity, due to their insulating nature.

They [49] also investigated the mechanical stability of the formed freeze linings. They found that some linings shattered on quenching and explained this with a combination of a phase transformation of dicalcium silicate within the freeze lining that causes a volume expansion of 12% and the thermal stresses that are caused during quenching. However, during the experiments, the lining temperatures were above the transformation temperature so that during the experiment, the lining was found to be stable. However, in industry, instead of air cooling, water cooling is usually employed, so that the minimum lining temperature will probably be lower than the transformation temperature, which could result in mechanical failure of the freeze lining. This is similar to the rhombohedric-to-monoclinic transformation in the cryolite system, which results in shattering of the lining upon cooling and the more practical result that the linings in the Hall Héroult process are operated above the corresponding temperature (563 °C) [61].

Fallah-Mehrjardi et al. [54] even investigated a molten fluoride salt bath, which is well known to have very low viscosities. In this case, the interface also consisted of a dense-sealing layer of the primary-phase cryolite (Na_3AlF_6). All these experiments further support the proposed mechanism. They also investigated this system later on [48] in more detail. Thonstad and Rolseth [7] and Solheim and Støen [41] had already investigated this system using both industrial and synthetic bath samples and concluded that the interface temperature depended on the solidification rate. They investigated the freeze linings with conventional light optical microscopy with reflected light. However, this technique is not able to distinguish the different phases from one another.

Fallah-Mehrjardi et al. [48] also investigated the microstructure more in depth. They found layers 2 (Glass-with-microcrystalites), 3 (Closed crystalline layer), 5 (Sealing primary-phase layer), and 7 (Residual bath). The older study by Solheim and Støen [41] showed that the deposit composition did not correspond to that of stoichiometric cryolite (the primary phase) with bulk chemical analysis. The BSE images made by Fallah-Mehrjardi et al. [48] showed that this non-stoichiometric composition is not related to occlusions or formation of other phases in the lining. No crystals of cryolite were observed by Fallah-Mehrjardi et al. [48] immediately next to the interface. The temperature profiles estimated using the thermocouples in the system, together with the observations of the present phases, showed that the interface temperature was equal to $T_{liquidus}$. The liquidus temperature and subliquidus equilibria they determined differed significantly from those previously reported in experimental studies. This different value for $T_{liquidus}$ sheds a different light on the previously reported superheats. They further noted that the bulk composition of the deposit-stayed constant, but that the phase assemblage could change over time when held at subsolidus temperatures. Hence, the final microstructure depends on the thermal history of the deposit.

It is noteworthy that Thonstad and Rolseth [7] also investigated the influence of the liquidus temperature of the system. The liquidus temperature of the cryolite–alumina bath can be lowered by using various additives, such as AlF_3, CaF_2, and LiF. These experiments were executed in a cold model system of a solution of stearic acid and myristic acid. Because the interface temperature was equal to the liquidus temperature in these experiments, a given change in the liquidus temperature should result in a corresponding change in the bath temperature, to keep the superheat constant. Hence, it was found that, as the liquidus temperature of the bath is changed, the bath temperatures shift in the same direction. This was attributed to the achievement of thermal balance.

Influence of Bath Agitation

Furthermore, the effects of bath agitation were also investigated in another study by Fallah-Mehrjardi et al. [55]. Again, the microstructure, morphology of the phases, and formation of various layers across the freeze lining were studied in steady-state conditions. The rotation speed of the crucible was changed, while all other parameters were kept fixed, and the first observation was that a higher rotation speed led to a higher heat input from the bath, resulting in much thinner freeze linings. The changes in the fluid flow pattern also influenced the microstructure. For the very fast rotation of the crucible, the dense-sealing layer of the primary phase was observed. This explicitly indicates that the interface temperature was higher for this system with faster crucible rotation. Furthermore, faster fluid flow at the interface decreases the crystal sizes during growth. If the interface temperature would have been at $T_{liquidus}$, no influence of fluid flow on the interface structure under steady-state conditions would have been expected, and only the primary phase would be present at the interface [60]. Note that Crivits et al. [32] concluded that differences in bulk fluid flow did not noticeably influence the low-temperature system. On the other hand, the phases formed, the interface temperatures, and the freeze-lining thicknesses were clearly highly sensitive to parameters that determine the chemical driving forces for change (bath temperature, bath composition, and thermal history of the deposit).

'Quantitative' Framework

Fallah-Mehrjardi et al. [60] also extended the conceptual framework from qualitative to semi-quantitative in a binary eutectic A–B system with no solid solution of B in A; hence, the primary phase is pure solid A and the solidus temperature is the eutectic temperature. In this more quantitative description, they focus on a cell of fluid material with composition X_{bath} which moves towards the interface and reaches the liquidus temperature at time step $t_0 = 0$. The crystallization starts and the amount of precipitated phase increases while the temperature further decreases to the interface temperature T_f. The deposition rate of A on the detached solids is given by $R(t)$ [mol/s] and the amount of material that gets deposited on the detached solids over a time t_f is ΔM_{Af}[moles] is $\int_{t_0}^{t_f} R(t)\,dt.$. This influences the mole fraction of B in the liquid as described in Eq. (11):

$$X_f = M_{B0}/(M_{B0} + M_{A0} - \Delta M_{Af}) = M_{B0}/(M_{B0} + M_{A0} - \int_{t_0}^{t_f} R(t)\,dt). \quad (11)$$

Because X_f will influence the interface temperature T_f, the crystallization extent will also clearly play its role. This extent of crystallization in turn depends on the crystallization kinetics, as illustrated by the presence of the term $R(t)$, and convection as illustrated by the presence of

the term t_f. They also introduced a 'mean crystallization rate' as $R_f = (\int_{t_0}^{t_f} R(t)\,dt)/t_f$. Hence, the extent of crystallization can be expressed by $R_f \cdot t_f$ where R_f describes the factors influencing the rate of crystallization and t_f is a function of the convective flow in the subliquidus layer next to the interface. This analysis was proposed by Fallah-Mehrjardi et al. [60] as a potential approach to the qualitative and future quantitative analysis of T_f and through that value, other properties. As most properties influencing the convective flow and crystallization rate lack actual values in the literature, the current application of this analysis remains qualitative but could still be very useful to make predictions on the limiting percent solids formed on equilibrium cooling, based on the phase diagram. Furthermore, it should be noted that the conceptual framework applies for steady-state conditions, in which the deposit/liquid interface velocity is zero.

Industrial Implications

The above-mentioned research has important implications for the pyrometallurgical industrial reactors. It means that certain process temperatures below $T_{liquidus}$ can be used. This could lead to a decrease in used energy and hence could save in operating cost. This subliquidus processing temperature will result in solid particles being present, but the above findings suggest that the chances for a catastrophic build-up of solids against the cooled reactor wall are very low [54, 60].

This was also demonstrated by Fallah-Mehrjardi et al. [52] in a nonferrous industrial slag with an industrial version of the air-cooled probe (in a slag pot filled with 3 tons of liquid lead blast furnace slag, as compared to the laboratory scale of 3.5 kg). The probe and the resulting deposit are shown in Fig. 11. Note that the observed glass layer contained spinel crystals, but these were also present in the bulk bath, which was operated at subliquidus temperatures. No sealing primary-phase layer was observed. This probe could be used to take bath samples from actual smelter operations, because it is air cooled and not water cooled (which would result in an inherent danger for vapor explosions). The study clearly showed the potential for forming stable steady-state freeze linings in metallurgical reactors operating below $T_{liquidus}$ of the slag, if the bulk flow conditions are controlled. This is because the deposit thickness remains unaltered due to the dynamic conditions present at the interface.

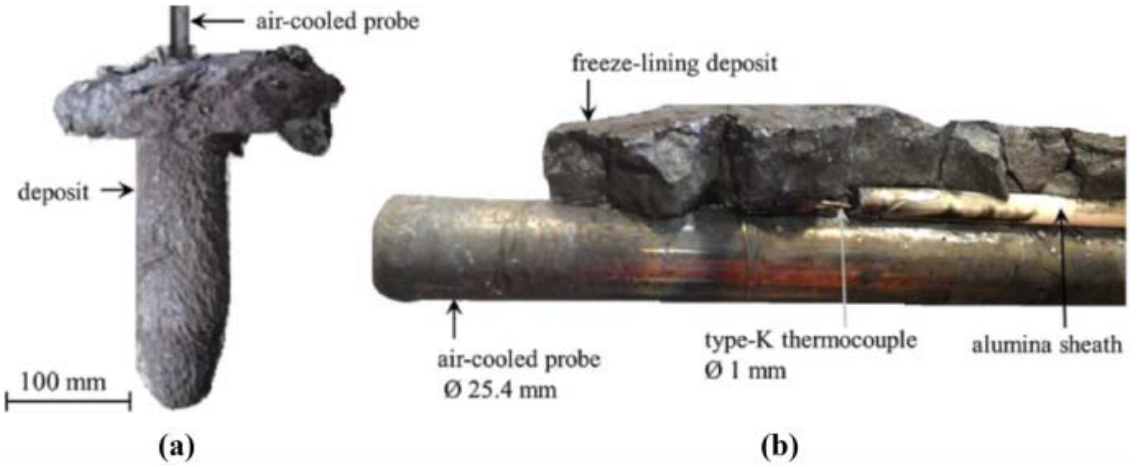

Fig. 11. Macro-images of the in situ deposit formed at bath temperature: 1473 K (1200 °C), air flow rate: 600 L/min, and immersion time: 0.5 h. Reprinted with permission from [52]

These findings were also supported by the laboratory experiments of Crivits et al. [53]. They found that when no detached crystals are observed, the primary phase was not present at the interface, even though thermal steady state was reached. They also measured the interface temperature, and these were, for all experiments, well below the estimated liquidus temperatures at thermal steady state in all of the conditions studied. Furthermore, even when the bulk liquid contained detached primary-phase crystals, these were not deposited on the interface. Hence, the conventional view of freeze linings (where all precipitated solids are deposited on the lining) was clearly not true.

Modeling

Most of the current knowledge regarding freeze linings is based on experience in primary metal processing industries in which the feed streams do not vary widely in composition, in contrast to metal recycling/secondary industries. To be able to use freeze linings also in secondary industries, it becomes critically important, to be able to, not only monitor and control the freeze-lining thickness but also to predict the influence of certain operational changes (which are inherent in secondary processing) on the freeze-lining thickness. For the latter, process modeling is required and can also help in understanding the governing mechanisms of the process and the freeze-lining formation.

Freeze-lining models in pyrometallurgical reactors can be subdivided into several categories based on the technique used to determine the position of the hot face (i.e., the freeze lining vs bath interface). The three categories are (1) models with strong numerical solutions (interface-tracking models), (2) models with weak numerical solutions (non-interface-tracking models), and (3) models using thermodynamic phase equilibrium calculations to determine the position of the hot face (macroscopic process models).

Interface-Tracking Models

The models using interface tracking to determine the position of the hot face have the particular feature that separate governing equations are solved in the solid and liquid phases and that the movement of the hot face is explicitly described by a separate mathematical equation. A mathematical boundary condition is required at the hot face so that the temperature or concentration fields can be solved separately in the solid and liquid phases; these models are often referred to as ‘moving boundary problems’ or ‘Stefan problems.’ They provide good insight in the phenomena present in the system but are limited in use for higher dimensions and multicomponent systems.

The first interface-tracking models described the steady-state temperature distributions of freeze linings. Robertson and Kang [30, 62] investigated heat transfer in the freeze lining of slag-cleaning furnaces through physical model studies and mathematical modeling. They used a one-dimensional thermal model equation that assumes a constant bath composition and thermal conductivity and a negligible heat accumulation in the wall. As such, the thickness of the freeze lining can be solved analytically. It is noteworthy to mention that the model assumed a hot-face temperature equal to the slag liquidus temperature.

Wei et al. [8] added transient heat transfer to a one-dimensional thermal model, to study the response of the bath and side ledge in Hall–Héroult cells on a changing alumina feed rate. They used a moving finite difference method to mathematically track the solidification front and solve the heat transfer equations. The grid superimposed on the sidewall was fixed, whereas

the grid superimposed on the ledge region was deformable in order to track the moving front. The bath and side ledge material were considered as a single component material with a melting point equal to the bath liquidus temperature and the thermal conductivity of the bath was assumed constant. Mass transport phenomena were ignored.

In later studies, the 'effective' liquidus temperature was used in this type of models [41, 63]. Here, the bath-freeze-lining interface temperature is equal to the liquidus temperature of the local liquid at the bath-freeze-lining interface. For a melting freeze lining, the effective liquidus temperature is higher than the liquidus temperature of the bath, while for a growing freeze lining, the effective liquidus temperature is lower than the liquidus temperature of the bath. As a result, the melting/growth of the freeze lining occurs more slowly than estimated by models that use the bath liquidus temperature in all cases. Therefore, mass transfer was also introduced in a one-dimensional model, because the local liquid composition is determined by the rates of heat transfer and mass transfer. For high solidification rates, the freeze-lining composition will be close to that of the bath, while for low solidification rates, the freeze-lining composition will be close to that of the primary phase [47].

The model is based on the simultaneous solution of equations for thermal conduction in bath and side ledge and for diffusion in the liquid phase. The freeze lining and the bath have different chemical compositions. Hence if the freeze-lining thickness changes, this must be accompanied by mass transfer besides heat transfer. During freezing, a bath constituent that is not incorporated in the lining will be enriched at the surface, and it must diffuse back to the bath. Solheim [9] proposed to use the Stefan-Maxwell equations to describe this multicomponent diffusion and also used turbulent diffusion coefficients because in the bulk of the bath, the heat and mass fluxes are determined by convection, but within the boundary layer at the interface, the convection decreases gradually and finally becomes zero at the interface, at which point the transport only depends on chemical diffusion and heat conduction. The turbulent quantities are described by a relation to the distance from the interface to the power 3. The model itself was one dimensional and had to make certain assumptions regarding values for the diffusion coefficients as these were 'the most uncertain data.' Furthermore, a correction factor was also included for the difference in composition between the lining and the bath in the rate of freezing, which improved the predictability of the numerical method. However, the model was only valid for low freezing rates, but this is the case for most practical industrial operations. This kind of models, incorporating mass transfer, were only developed for the freeze-lining behavior of cryolite salt in the Hall–Héroult process for which experimental data were available.

Non-interface-Tracking Models

In other models, the moving interface is not tracked explicitly but follows implicitly by solving one set of equations for the domain as a whole. These models are easier to implement in multiple dimensions and can be easily extended to multi-dimensional geometries. Furthermore, no boundary conditions are required at the hot face. The drawback of these models is that the exact position of the hot face is not known, but this can be derived from the position of certain grid cells that are partially filled with solid and liquid phases.

Scholey et al. [64] investigated the water-cooled zinc-fuming jackets with a one-dimensional model that describes the transient heat transfer, while assuming a constant bath composition and constant slag properties as a function of temperature. The equations for transient thermal conduction are solved mathematically, and the release of latent heat was modeled by increasing

the heat capacity in the temperature range between solidus and liquidus in a 'sinusoidally varied—constant value' composite way, which could be best described by a topped-off parabolic function. The increased heat transfer in the bath due to stirring was taken into account by artificially increasing the thermal conductivity of the bath. Extensions to two dimensions have been developed to investigate the steady-state temperature distribution, side ledge profile, influence of slag fall-off, and design effects in the Hall-Héroult process [65, 66].

Campbell [67] used Computational Fluid Dynamic (CFD) modeling coupled to thermo-mechanics to investigate refractory wear and freeze-lining formation. The model is two dimensional and assumes constant bath composition during solidification. The solidification itself was implemented in the model by adding source terms in the energy and momentum equations. A Darcy source term is applied to the momentum calculations in the regions where solid materials are found, such as refractory. By this approach, the slag is able to take up the worn refractory volumes. Additionally, an energy source term is added to the heat transfer equations to account for the solidification that is occurring. It was even possible to predict the refractory wear that occurs prior to the freeze-lining formation. The model was used to investigate the influence of the process conditions on the freeze lining and refractory wear. The refractory wear mechanisms described here were a simplification as it was assumed that the refractory is a homogenous material. In reality, refractory has a complex crystalline structure, and this mineralogy can significantly influence in the performance under process conditions.

Later, Guevara et al. [36] also used a non-interface-tracking model with temperature-dependent viscosity and density functions. They assumed the interface temperature to be equal to the solidus temperature, as they observed this during their experiments [35]. To suppress velocities in the solid phase, various model approaches were compared:

- The enthalpy-porosity model: assumes the flow in the dendritic region is like flow through a fixed bed of porous media and is governed by Darcy's law. This assumption allows the computation of flow resistance for liquid passing through the evolving microstructure. In the Enthalpy-Porosity model, a damping function factor is added in the momentum equations in the form of a source term. This source term dominates the transient convective and diffusive terms, and the momentum equation approximates Darcy's law. As the local solid fraction approaches unity, the source term dominates all other terms forcing the velocities to approach zero. This addition of a Darcy source term was also used in the CFD modelling of Campbell [67].
- A high viscosity value is set for the solid phase. This approach has not been used often. Originally, the rule of mixtures was proposed for the viscosity of the two-phase zone, i.e., a linear relationship between solid viscosity and liquid viscosity.

They found that the use of a high effective viscosity was most appropriate. The best agreement with experiments was achieved with a harmonic relationship. It was also essential that temperature-dependent viscosity relationships for the liquid are used. Their simulations [36] agreed well with the results from their own experiments in a cold apparatus [35].

Macroscopic Process Models

In macroscopic process models, both the bath chemistry and freeze-lining behavior are described in the same approach. The position of the solidification front is calculated from solid–liquid equilibrium calculations with thermodynamic software. The main advantage of these

models is that the effects of operational conditions and process chemistry on the freeze lining can be investigated.

For the ilmenite smelting process, Pistorius [59] proposed an approximately one-dimensional pseudo-steady-state process model that was a combination of the one-dimensional heat transfer through each layer and free energy minimization to calculate local equilibrium at the interface between the slag and metal bath.

Pistorius [59] used the model to investigate whether the freeze-lining mechanism may force the bath composition close to a eutectic groove of the ilmenite phase diagram. The model is based on solidification equilibria, combined with a simple heat transfer model to quantify heat loss through the freeze lining. They used a series of polynomial expressions to describe the shapes of the phase boundaries on the ternary phase diagram, obtained from the thermodynamic software Factsage. Furthermore, the expressions for the enthalpy data were represented by simplified expressions, fitted to the values from the thermodynamic software. Due to lack of experimental data on Ti-rich slags, a constant value of 1 W/(K m) for the thermal conductivity was assumed for the freeze lining [59], and the molar densities of the freeze lining and slag were assumed to be equal.

The heat transfer model was then combined with a mass and energy balance to investigate how the freeze lining reacted to certain 'disturbances' such as adding slag to the system or changes in the power input into the bath. The model includes the description of chemical reactions in the process as it is assumed that the freeze lining is formed by deposition of the equilibrium solids present in the bath. He modeled the dynamic response of the slag and freeze lining to different inputs (flow rates of ilmenite and reductant, and power input). Pistorius [59] concluded that the freeze-lining mechanism cannot force the bath composition close to a eutectic groove in the phase diagram and, therefore, could not explain the observed slag compositional invariance.

The simplified approach (it assumes full equilibrium between the liquid slag and the freeze lining) neglects many of the complexities that arise in actual furnaces, i.e., temperature and compositional heterogeneities within the phases, diffusion through the solid, 2-dimensional heat transfer and the details of chemical reactions. Furthermore, the contact between the metal and freeze lining was not considered. However, the results clearly showed that a freeze lining in an ilmenite smelter can melt away rapidly (a too high heat flux can melt away the freeze lining in a few minutes), but that regrowth of the lining is a much slower process (it takes hours to rebuild a freeze lining after it has been lost). Furthermore, it became clear that changes of the input into the slag bath (slag composition and power) have a direct effect on the freeze lining.

This work was further extended by Zietsman [68] to study interactions between the slag bath and the freeze lining. The 1D Wall Model was developed to describe one-dimensional radial heat transfer in the freeze lining and furnace sidewall, and melting and solidification at the freeze-lining hot face. This work was the basis for proposing a mechanism that successfully explains the compositional invariance observed in ilmenite smelting slags. These slags consist predominantly of a single pseudobrookite phase [69].

Zietsman and Pistorius [70] also applied the model to investigate how severe operational errors (losing all feed, only all reductant or only all ilmenite) influences the freeze lining. They concluded that these severe errors should be avoided if possible, or if detected, as quick as

possible action is required to counter the effect. If the error is detected early, it may be sufficient to stop all process inputs, most importantly electrical power, so that the extra energy discharged into the process gets dissipated to the freeboard, metal bath, and freeze lining. So that, hopefully, the entire freeze lining would not melt away. If the error was not detected early, the slag can be superheated significantly, but switching off the furnace entirely may not be enough to protect it. The superheated slag will continue to dissolve the freeze-lining and refractory material. In such case, the two largest process heat sinks should be used: the heating and melting of ilmenite and the reduction reactions at the reductant–slag interface.

Verscheure et al. [10, 19, 21] developed a mathematical model for the Zn-fuming process that combined thermodynamics, phase equilibria in the process, activities of the species in each phase, heat transfer in the process, and the behavior of the freeze lining. Note that the heat balance was only evaluated at the hot face of the freeze lining, and the temperature of this hot face of the freeze lining was assumed to be the liquidus temperature of the slag. The overall process was split up in a sequence of four reaction stages which were all assumed to attain thermodynamic equilibrium. The model incorporates a steady-state description of the freeze lining, with its behavior largely governed by the solid–liquid phase transition of the slag phase. The model can be used to analyze the relative effects of various parameters of the zinc-fuming processes and to provide valuable information for the optimization of the operational characteristics including carbon, electrical power, and feed rate. This model was then applied to the submerged-plasma zinc-fuming process to investigate the sensitivity to changing process conditions as compared to the base case compiled from the pilot plant trials performed by Umicore on their 750 kg/h reactor. Furthermore, the comparison to the conventional zinc-fuming process was made, which indicated that the submerged-plasma process has a 4.6 times higher fuming rate than the conventional process [20].

Pan et al. [71] investigated the heat transfer in an electrical furnace with six in-line electrodes, used for smelting sulfide ores to produce base metals and platinum group metals. They also took a freeze lining into account, but this was not the main point of focus. It is a steady-state model focusing mostly on heat transfer and relates input and control parameters to the furnace conditions and performance. Several assumptions and simplifications were made, to keep the calculation times limited to a few seconds. Their assumptions include uniform heat dissipation and independent consideration of thermal and chemical reaction effects. Furthermore, they assume that the interface between the slag and freeze lining has a temperature equal to the solidus temperature. The model was able to predict the temperature profile in the system, the freeze-lining thickness, and the process efficiency. Due to the low execution time, it is possible to use the model for online prediction and control of heat transfer and freeze-lining thickness in industrial electric furnaces.

Conclusion and Outlook

It became clear over time that not only thermal considerations are important for freeze-lining formation, but that the viscosity relative to flow velocity also plays a major role. The formation of freeze linings is complex and depends on a combination of slag properties (viscosity or the ability to flow and diffusivity or the distribution speed of components) and elementary process steps (nucleation, crystallization, and dissolution kinetics), in addition to the convective flow patterns and diffusion processes in the liquid bath. As previous work did not investigate the relationships between solid fraction and temperature, and between solid fraction and enthalpy, this review also did not emphasize them. However, these factors could also explain certain

differences in solidification behavior between different systems and should, therefore, be investigated more thoroughly in the future.

There is a clear need for further systematic investigation of various parameters that influence these systems under dynamic conditions. For this, both experiments and models are required. The next sections give a summary of the remaining challenges and future work on freeze lining, from an experimental and modeling approach.

Experimental

Crivits et al. [53] listed the possible causes for the remaining uncertainties in the calculated thermal conductivities of the freeze linings resulting from their laboratory experiments using a cooled probe (in the CuO_x-FeO_y-MgO-SiO_2 system at copper metal saturation):

- Geometry: linings being modeled as a combination of a cylinder and half a sphere
- Metallic content: thermal conductivities of the oxide system and metal differ significantly so that a small change in metallic content greatly influences the determined thermal conductivity.
- Coolant flow rate: the air flow rate was controlled within ± 5 L/min but resulted in an uncertainty of ± 5% in the calculated thermal conductivities.
- Depth probe/bath level: the bath level was estimated before the experiment but turned out to be lower. This creates an extra radiative heat factor at certain points, influencing the temperatures measured at the inlet and outlet of the coolant.
- Ridge formation: a ridge can be formed that does not connect to the cold probe but can influence the heat transfer in the system.
- Freeze-lining temperature profile: there is only a limited number of temperature measurements in the lining, so that the estimated temperature profile can differ somewhat. The resulting uncertainty on the thermal conductivity was estimated to be within 10%.
- Furnace type: freeze linings investigated in an electrical furnace had thermal conductivities estimated an order of magnitude less than those measured with an induction furnace. This difference was marked as unexplainable. However, we raise the question whether the metal droplet content could be relevant here.
- Bath temperature: bath temperature was assumed constant, but in reality temperature, gradients could be present in the bath.
- Interface morphology: different interface morphologies may result in different local fluid flow, and thus also in different heat and mass transfer.

More general recommendations are to investigate thinner freeze linings in a system where no metallic phase is formed, with a deeper probe immersion and using only one kind of furnace. Better attention should be paid on the thermocouple position and the bath temperature should be controlled, instead of using a constant furnace generator power [53].

Furthermore, it is clear that the viscosity is a very important physical parameter, which has a complex influence on the freeze-lining formation. The reason for this is the dependence of a lot of parameters on the viscosity: mass diffusion, boundary layer thickness, convective flow, nucleation, solidification, etc. All these phenomena play a role in freeze-lining behavior; however, the interactions in between have not yet been established. [49] Being such an important influencing parameter, a clear need is present for more and reliable viscosity experiments and predictive models. It should be noted that more and better data are also

required for the other influencing parameters such as thermal properties and chemical properties

Modeling

As most models until now assumed an interface temperature equal to the liquidus temperature, with one exception choosing the solidus temperature, they are clearly limited. Furthermore, the previous models mostly focused on the thermal aspects and some of them combined this with process/chemical aspects of the freeze lining, but a model which also takes into account the flow within the reactor, which is also a very important influencing parameter, and the formed microstructure, which is essential for the stability of the freeze lining, has not been proposed yet. A distinction should be made between models considering the macroscopic scale of the process and the more fundamental models incorporating microstructure formation.

In the former category (models considering the macroscopic scale of the process), Zietsman et al. [72] investigated the influence of a set of DC furnace design and operating parameters on slag freeze-lining behavior in open-bath ilmenite- and chromite-smelting furnaces. This was done via CFD simulations in OpenFOAM [73], describing energy transport, fluid flow, arc momentum transfer, and liquid-to-solid phase change based on localized thermochemical equilibria. However, the model used approximations in which the energy absorbed by reduction reactions was ignored and assumed the slag bath to freeboard interface to be thermally insulating. The phase change model describes the formation and transportation of a mushy zone and allows for the treatment of changing material properties between the solid and liquid phases, including density, heat capacity, and thermal conductivity. Flow resistance during solidification was accounted for by a viscosity change model. They are able to investigate bath diameter, energy intensity (also called hearth power density), sidewall refractory material selection, electrical power and resistance, slag and alloy bath depths, and slag chemical composition and the associated slag thermophysical properties.

In the latter category (more fundamental models incorporating microstructure formation), no such model exists yet, but it would be valuable to simulate the influence of the process history on the microstructure in combination with the flow as well. Hence, clearly, a lot of room for improvement regarding modeling freeze linings is available.

Notes

1. For crystallization to take place, the temperature should be sufficiently low, at least below the liquidus temperature, not only to have sufficient crystal nucleation, but also sufficiently high to permit fast enough kinetics for the crystals to grow. Note, that there is also another lower limit: the glass transition temperature. At this temperature, the mobility of the atoms strongly decreases during cooling. However, because liquid slag may be highly viscous above the glass transition temperature, crystallization can also be limited at higher temperatures [42].

Acknowledgements

Bellemans holds a research grant from the Research Foundation Flanders (12Z7720N).

On behalf of all authors, the corresponding author states that there is no conflict of interest.

References

1. Malfliet A et al (2014) Degradation mechanisms and use of refractory linings in copper production processes: a critical review. J Eur Ceram Soc 34(3):849–876
2. Hearn AM, Dzermejko AJ, Lamont PH (1998) 'Freeze' lining concepts for improving submerged arc furnace lining life and performance. In: 8th international ferroalloys congress, pp 401–426
3. Verscheure K, Kyllo AK, Filzwieser A, Blanpain B, Wollants P (2006) Furnace cooling technology in pyrometallurgical processes. In: 2006 TMS fall extraction and processing division: Sohn international symposium, vol 4, pp 139–154
4. Warczok A, Utigard TA (1993) Determination of the heat transfer coefficient between liquid fayalite slags and solid metal. Scand J Metall 22:68–74
5. Nelson LR, Hundermark RJ (2014) 'The tap-hole'-key to furnace performance. In: Furnace tapping conference 2014, p 32
6. Solheim A, Thonstad J (1984) Model experiments of heat transfer coefficients between bath and side ledge in aluminum cells. JOM 36(3):51–55
7. Thonstad J, Rolseth S (1982) Equilibrium between bath and side ledge in aluminium cells. Basic principles. In: Andersen JE (ed) Light metals 1982, The Minerals, Metals & Materials Society, Warrendale, PA, pp 415–524
8. Wei CC, Chen JJJJ, Welch BJ, Voller VR (1997) Modelling of dynamic ledge heat transfer. In: Huglen R (ed) Light metals 1997, The Minerals, Metals & Materials Society, Warrendale, PA, pp 309–316
9. Solheim A (2011) Some aspects of heat transfer between bath and sideledge in aluminium reduction cells. In: Lindsey SJ (ed) Light metals 2011, Springer, Cham, pp 381–386
10. Verscheure K, Van Camp M, Blanpain B, Wollants P, Hayes P, Jak E (2006) Freeze linings in zinc fuming processes. In: 2006 TMS fall extraction and processing division: Sohn international symposium, vol 1, pp 361–374
11. Pistorius PC, Coetzee C (2003) Physicochemical aspects of titanium slag production and solidification. Metall Mater Trans B 34:581–588
12. Maharajh S, Muller J, Zietsman JH (2015) Value-in-use model for chlorination of titania feedstocks. J South Afr Inst Min Metall 115(5):385–394
13. Heimo J, Jokilaakso A, Kekkonen M, Tangstad M, Støre A (2019) Thermal conductivity of titanium slags. Metall Res Technol Technol 116(6):10
14. Pistorius PC (2003) Fundamentals of freeze lining behaviour in ilmenite smelting. J S Afr Inst Min Metall 103(8):509–514
15. Hearn AM, Van Rensburg ASJ, Henning JR (2004) 'Freeze' lining on M12 furnace: motivation, installation and operation. In: INFACON X transformation through technology, pp 500–507
16. Kojo IV, Jokilaakso A, Hanniala P (2000) Flash smelting and converting furnaces: a 50 year retrospect. JOM 52(2):57–61
17. Duncanson PL, Toth JD (2004) The truths and myths of freeze lining technology for submerged arc furnaces. INFACON X transformation through technology, pp 488–499
18. Nelson LR et al (2004) Application of a high-intensity cooling system to DC-arc furnace production of ferrocobalt at Chambishi. J S Afr Inst Min Metall 104(9):551–561
19. Verscheure K, Van Camp M, Blanpain B, Wollants P, Hayes P, Jak E (2007) Continuous fuming of zinc-bearing residues: Part I. Model development. Metall Mater Trans B 38(1):13–20

20. Verscheure K, Van Camp M, Blanpain B, Wollants P, Hayes P, Jak E (2007) Continuous fuming of zinc-bearing residues. Part II: the submerged-plasma zinc-fuming process. Metall Mater Trans B 38(1):21–33
21. Verscheure K, Van Camp M, Blanpain B, Wollants P, Hayes PC, Jak E (2005) Investigation of zinc fuming processes for the treatment of zinc-containing residues. In: John Floyd international symposium on sustainable developments in metals processing
22. Davenport WG, King M, Schlesinger M, Biswas AK (2002) Extractive metallurgy of copper. Elsevier, Amsterdam
23. Fallah-Mehrjardi A, Jansson J, Taskinen P, Hayes PC, Jak E (2014) Investigation of the freeze-lining formed in an industrial copper converting calcium ferrite slag. Metall Mater Trans B 45(3):864–874
24. Taskinen P, Kaskiala M, Miettinen K, Jansson J (2013) Freeze-lining formation and microstructure in a direct-to-blister flash smelting slag. J Manuf Sci Prod 13(1–2):77–83
25. Swinbourne D (2010) The extractive metallurgy of lead. Miner Process Extr Metall 119(3):182
26. Vanparys R et al (2020) Reduction of lead-rich slags with coke in the lead blast furnace. In: Siegmund A et al (eds) PbZn 2020: 9th international symposium on lead and zinc processing, Springer, Cham, pp 173–185
27. Steenkamp H, Garbers-Craig AM (2020) An investigation into the permeability of a PGM slag freeze lining to sulphur. J S Afr Inst Min Metall 120:361–368
28. Shaw A et al (2013) Challenges and solutions in PGM furnace operation: High matte temperature and copper cooler corrosion. J S Afr Inst Min Metall 113(3):251–261
29. Jansson J, Taskinen P, Kaskiala M (2015) Microstructure characterisation of freeze linings formed in a copper slag cleaning slag. J Min Metall Sect B Metall 51(1):41–48
30. Robertson DGC, Kang S (1999) Model studies of heat transfer and flow in slag-cleaning furnaces. In: Fluid flow phenomena in metals processing, pp 157–168
31. Fallah-Mehrjardi A, Hayes PC, Jak E (2014) Understanding slag freeze linings. JOM 66(9):1654–1663
32. Crivits T, Hayes PC, Jak E (2018) An investigation of factors influencing freeze lining behaviour. Miner Process Extr Metall 127(4):195–209
33. Jansson J, Taskinen P, Kaskiala M (2014) Freeze lining formation in continuous converting calcium ferrite slags. II. Can Metall Q 53(1):11–16
34. Verscheure K et al (2006) Water-cooled probe technique for the study of freeze lining formation. Metall Mater Trans B 37(6):929–940
35. Guevara FJ, Irons GA (2011) Simulation of slag freeze layer formation: Part I experimental study. Metall Mater Trans B 42(4):652–663
36. Guevara FJ, Irons GA (2011) Simulation of slag freeze layer formation: Part II: numerical model. Metall Mater Trans B 42(4):664–676
37. Banerjee SK, Irons GA (1992) Physical modelling of thermal stratification, bottom build-up and mixing in submerged arc electric smelting. Can Metall Q 31(1):31–40
38. Campforts M et al (2006) Slag solidification with water-cooled probe technique. In: 2006 TMS Fall TMS extraction and processing division: Sohn international symposium, pp 309–321
39. Fallah-Mehrjardi A, Hayes PC, Jak E (2013) Investigation of freeze-linings in copper-containing slag systems: Part I. Preliminary experiments. Metall Mater Trans B 44(3):534–548
40. Taylor MP, Welch BJ (1987) Melt/freeze heat transfer measurements in cryolite-based electrolytes. Metall Trans B 18(2):391–398

41. Solheim A, Stoen LIR (1997) On the composition of solid deposits frozen out from cryolitic melts. In: Huglen R (ed) Light metals 1997, The Minerals, Metals & Materials Society, Warrendale, PA, pp 325–332
42. Campforts M, Jak E, Blanpain B, Wollants P (2009) Freeze-lining formation of a synthetic lead slag: Part I. Microstructure formation. Metall Mater Trans B 40(5):619–631
43. Campforts M, Blanpanin B, Wollants P (2009) The importance of slag engineering in freeze-lining applications. Metall Mater Trans B 40(5):643–655
44. Campforts M, Verscheure K, Boydens E, Van Rompaey T, Blanpain B, Wollants P (2007) On the microstructure of a freeze lining of an Industrial Nonferrous Slag. Metall Mater Trans B 38(6):841–851
45. Jansson J, Taskinen P, Kaskiala M (2014) Freeze lining formation in continuous converting calcium ferrite slags. I. Can Metall Q 53(1):1–10
46. Kalliala O, Kaskiala M, Suortti T, Taskinen P (2015) Freeze lining formation on water cooled refractory wall. Trans Inst Min Metall Sect C Miner Process Extr Metall 124(4):224–232
47. Campforts M, Jak E, Blanpain B, Wollants P (2009) Freeze-lining formation of a synthetic lead slag: Part II. Thermal history. Metall Mater Trans B 40(5):632–642
48. Fallah-Mehrjardi A, Hayes PC, Jak E (2014) Investigation of freeze-linings in aluminum production cells. Metall Mater Trans B 45(4):1232–1247
49. Crivits T, Hayes PC, Jak E (2018) Freeze linings in the Al_2O_3–CaO–SiO_2 system. Int J Mater Res 109(7):638–653
50. Van Winkel S, Scheunis L, Crivits T, Blanpain B, Malfliet A (2019) Microstructural changes in freeze linings during zinc fuming processes. In: Proceedings of the 6th international slag valorisation symposium, KU Leuven, Materials Engineering, pp 333–336
51. Campforts M, Verscheure K, Boydens E, Van Rompaey T, Blanpain B, Wollants P (2008) On the mass transport and the crystal growth in a freeze lining of an industrial nonferrous slag. Metall Mater Trans B 39(3):408–417
52. Fallah-Mehrjardi A, Hayes PC, Vervynckt S, Jak E (2014) Investigation of freeze-linings in a nonferrous industrial slag. Metall Mater Trans B 45(3):850–863
53. Crivits T, Hayes PC, Jak E (2018) Investigation of the effect of bath temperature on the bath-freeze lining interface temperature in the CuO_x-FeO_y-MgO-SiO_2 system at copper metal saturation. Int J Mater Res 109(5):386–398
54. Fallah-Mehrjardi A, Hayes PC, Jak E (2013) Investigation of freeze linings in copper-containing slag systems: Part II. Mechanism of the deposit stabilization. Metall Mater Trans B 44(3):549–560
55. Fallah-Mehrjardi A, Hayes PC, Jak E (2013) Investigation of freeze lining in copper-containing slag systems: Part III. High-temperature experimental investigation of the effect of bath agitation. Metall Mater Trans B 44(6):1337–1351
56. Crivits T, Hayes PC, Jak E (2015) Investigation of freeze linings in magnesia-containing copper slags. In: COM 2015: 54th annual conference of metallurgists, p 10
57. Eisenhuttenleute VD (1995) Slag atlas. Verlag Stahleisen
58. Mills KC, Su Y, Fox AB, Li Z, Thackray RP, Tsai HT (2005) A review of slag splashing. ISIJ Int 45(5):619–633
59. Pistorius PC (2004) Equilibrium interactions between freeze lining and slag in ilmenite smelting. J S Afr Inst Min Metall 104(7):417–422
60. Fallah-Mehrjardi A, Hayes P, Jak E (2014) Further experimental investigation of freeze-lining/bath interface at steady-state conditions. Metall Mater Trans B 45(6):2040–2049

61. Grjotheim K, Welch BJ (1988) Aluminium smelter technology: a pure and applied approach. Aluminum-Verlag, Germany
62. Kang S (1991) A model study of heat transfer and fluid flow in slag-cleaning furnaces. PhD Dissertation, University of Missouri
63. Solheim A (2003) Coupled heat and mass transfer during melting or freezing of side ledge in aluminium cells. In: 12th aluminium symposium
64. Scholey KE, Richards GG, Samarasekera IV (1991) Heat-transfer phenomena in water-cooled zinc-fuming furnace jackets. Metall Trans B 22(2):163–175
65. Bruggeman J, Danka D (1990) Two-dimensional thermal modeling of the Hall-Heroult cell. In: Light metals 1990, The Minerals, Metals & Materials Society, Warrendale, pp 203–209
66. Valles A, Lenis V (1990) Prediction of ledge profile in Hall-Heroult cells. In: Light metals 1990, The Minerals, Metals & Materials Society, Warrendale, pp 309–313
67. Campbell AP, Pericleous KA, Cross M (2002) Modelling of freeze layers and refractory wear in direct smelting processes. In: Proceedings—ironmaking conference, pp 479–491
68. Zietsman JH (2004) Interactions between freeze lining and slag bath in ilmenite smelting. PhD Thesis, University of Pretoria
69. Zietsman J, Pistorius PC (2004) Process mechanisms in ilmenite smelting. J S Afr Inst Min Metall Dec:653–660
70. Zietsman JH, Pistorius PC (2006) Modelling of an ilmenite-smelting DC arc furnace process. In: Minerals engineering, vol 19, no 3 SPEC. ISS, pp 262–279
71. Pan Y, Sun S, Jahanshahi S (2011) Mathematical modelling of heat transfer in six-in-line electric furnaces for sulphide smelting. J S Afr Inst Min Metall 111:717–732
72. Zietsman J, Bogaers A, Reynolds QG (2020) Freeze lining behaviour in DC smelting furnaces: the influence of furnace design and operation. Presented at The 11th molten slags, fluxes and salts [MOLTEN 2020], Seoul, Korea
73. “OpenFOAM.” https://www.openfoam.com